Lithos 126 (2011) 248–264

Contents lists available at ScienceDirect

Lithos

journal homepage: www.elsevier.com/locate/lithos

Zircon U–Pb ages, Hf–O isotopes and whole-rock Sr–Nd–Pb isotopic geochemistry of granitoids in the Jinshajiang suture zone, SW China: Constraints on petrogenesis and tectonic evolution of the Paleo-Tethys Ocean

Jing-Jing Zhu [a,b], Rui-Zhong Hu [a,*], Xian-Wu Bi [a], Hong Zhong [a], Heng Chen [a,b]

[a] State Key Laboratory of Ore Deposit Geochemistry, Institute of Geochemistry, Chinese Academy of Sciences, Guiyang 550002, China
[b] The Gradute School of the Chinese Academy of Sciences, Beijing 100039, China

ARTICLE INFO

Article history:
Received 3 May 2011
Accepted 14 July 2011
Available online 22 July 2011

Keywords:
I-type granite
Zircon U–Pb dating
Zircon Hf–O isotope
Sr–Nd–Pb isotope
Three-component mixing
Paleo-Tethys Ocean

ABSTRACT

The Jinshajiang suture zone, located in the eastern part of the Tethyan tectonic domain, is noticeable for a large-scale distribution of Late Jurassic to Triassic granitoids. These granitoids were genetically related to the evolution of the Paleo-Tethys Ocean. Beiwu, Linong and Lunong granitoids occur in the middle zone of the Jinshajiang Suture Zone, and possess similar geochemical features, indicating that they share a common magma source. SIMS zircon U–Pb dating reveals that the Beiwu, Linong and Lunong granitic intrusions were emplaced at 233.9 ± 1.4 Ma (2σ), 233.1 ± 1.4 Ma (2σ) and 231.0 ± 1.6 Ma (2σ), respectively. All of these granitoids are enriched in abundances of Si (SiO_{2t} = 65.2–73.5 wt.%), and large-ion lithophile elements (LILEs), but depleted in high field strength elements contents (HFSEs, e.g., Nb, Ta, and Ti). In addition, they have low P_2O_5 contents (0.06–0.11 wt.%), A/CNK values ([molecular Al_2O_3/($CaO + Na_2O + K_2O$)], mostly < 1.1) and 10,000 Ga/Al ratios (1.7–2.2), consistent with the characteristics of I-type granites. In terms of isotopic compositions, these granitoids have high initial $^{87}Sr/^{86}Sr$ ratios (0.7078–0.7148), Pb isotopic compositions [($^{206}Pb/^{204}Pb)_t$ = 18.213–18.598, ($^{207}Pb/^{204}Pb)_t$ = 15.637–15.730 and ($^{208}Pb/^{204}Pb)_t$ = 38.323–38.791], zircon $\delta^{18}O$ values (7.3‰–9.3‰) and negative $\varepsilon_{Nd}(t)$ values (−5.1 to −6.7), suggesting they were predominantly derived from the continental crust. Their Nb/Ta ratios (average value = 8.6) are consistent with those of the lower continental crust (LCC). However, variable $\varepsilon_{Hf}(t)$ values (−8.6 to +2.8) and the occurrences of mafic microgranular enclaves (MMEs) suggest that mantle-derived melts and lower crustal magmas were involved in the generation of these granitoids. Moreover, the high Pb isotopic ratios and elevated zircon $\delta^{18}O$ values of these rocks indicate a significant contribution of the upper crustal composition. We propose a model in which the Beiwu, Linong and Lunong granitoids were generated under a late collisional or post-collisional setting. It is possible that this collision was completed before Late Triassic. Decompression induced mantle-derived magmas to be underplated and provided the heat for the anatexis of the crust. Hybrid melts including mantle-derived and the lower crustal magmas were then generated. The hybrid melts thereafter ascended to a shallow depth and resulted in some degree of sedimentary rock assimilation. Such three-component mixing magma source and subsequent fractional crystallization could be responsible for the formation of the Beiwu, Linong and Lunong granitoids.

1. Introduction

As widely accepted (Wu, et al., 2007; Wyllie, 1977; Zhang et al., 2008b), most granites are of crustal origin. The majority of I- and S-type granites in the continental crust are considered to be derived from preexisting infracrustal igneous rocks and supracrustal sedimentary rocks (Li et al., 2009a; White and Chappell, 1977). However, recent studies indicate mantle-derived magma input might be inevitable for most granites, and mantle-derived magmas were even involved in the generation of some strongly peraluminous S-type granites and rhyolites (Clemens, 2003; Kemp et al., 2007; Li et al., 2009a; Sylvester, 1998). Apparently, it is significant to identify these components associated with mixing of magmas. In general, geochemical and Sr–Nd–Pb isotopic data were proposed for identifying mantle-derived and crustal compositions, however, it is usually difficult to provide satisfactory evidence due to their uncertain interpretations (Chappell et al., 1987; Chappell and White, 1992; Kemp, et al., 2007; Li et al., 2009a). Oxygen isotopes of zircon can provide an effective constraint on the involvement of mantle-, upper crust- and lower crust-derived magmas in the genesis of granites (Kemp, et al., 2007; Lackey et al., 2005; Valley et al., 2005; Zheng et al., 2007). Zircon has high oxygen isotope closure temperature, which is

* Corresponding author. Tel.: +86 851 589 1962; fax: +86 851 589 1664.
E-mail address: huruizhong@vip.gyig.ac.cn (R.-Z. Hu).

0024-4937/$ – see front matter © 2011 Elsevier B.V. All rights reserved.
doi:10.1016/j.lithos.2011.07.003

not to be reset even if the mineral underwent granulite-facie metamorphism (King et al., 1998; Valley et al., 1994). Thus, oxygen isotopes of zircon preserve the features of magma sources. Mantle-derived magmas ($\delta^{18}O$ value = 5.3‰ ± 0.3‰; King et al., 1998; Valley et al., 1998), the lower crustal granulite-facies igneous rocks ($\delta^{18}O$ value = 7‰; Pamela et al., 1992), and the supracrustal magmas ($\delta^{18}O$ value = 10‰–30‰; Valley et al., 2005) have distinct O isotopes. Zircon Hf isotopes provide another approach to trace the origin of granites. Because zircons have high Hf concentrations (generally about 10,000 ppm or 1%), low Lu/Hf ratios (~<0.01) and resistance to isotopic disturbance (Goodge and Vervoort, 2006), they can preserve details of isotopic variations during the mixing of the different magmas (Griffin et al., 2002; Li et al., 2009a). Therefore, combined with geochemical and Sr–Nd–Pb isotopic data, zircon Hf–O isotopes can provide important constraints on the origin of granites.

The Sanjiang Domain (SD) in southwestern China is located in the eastern part of the Tethyan–Himalayan tectonic belt, and also in the tectonic junction between Gondwanaland and Eurasia (Hou et al., 2003; Li et al., 1999; Li and Jiang, 2003; Lü et al., 1993; Mo et al., 1993). Several of the Paleozoic sutures in the region provide a record of the history of the Paleo-Tethys Ocean, which consists of four paleo-oceanic basins: the Garze–Litang, Jinshajiang, Lancangjiang and

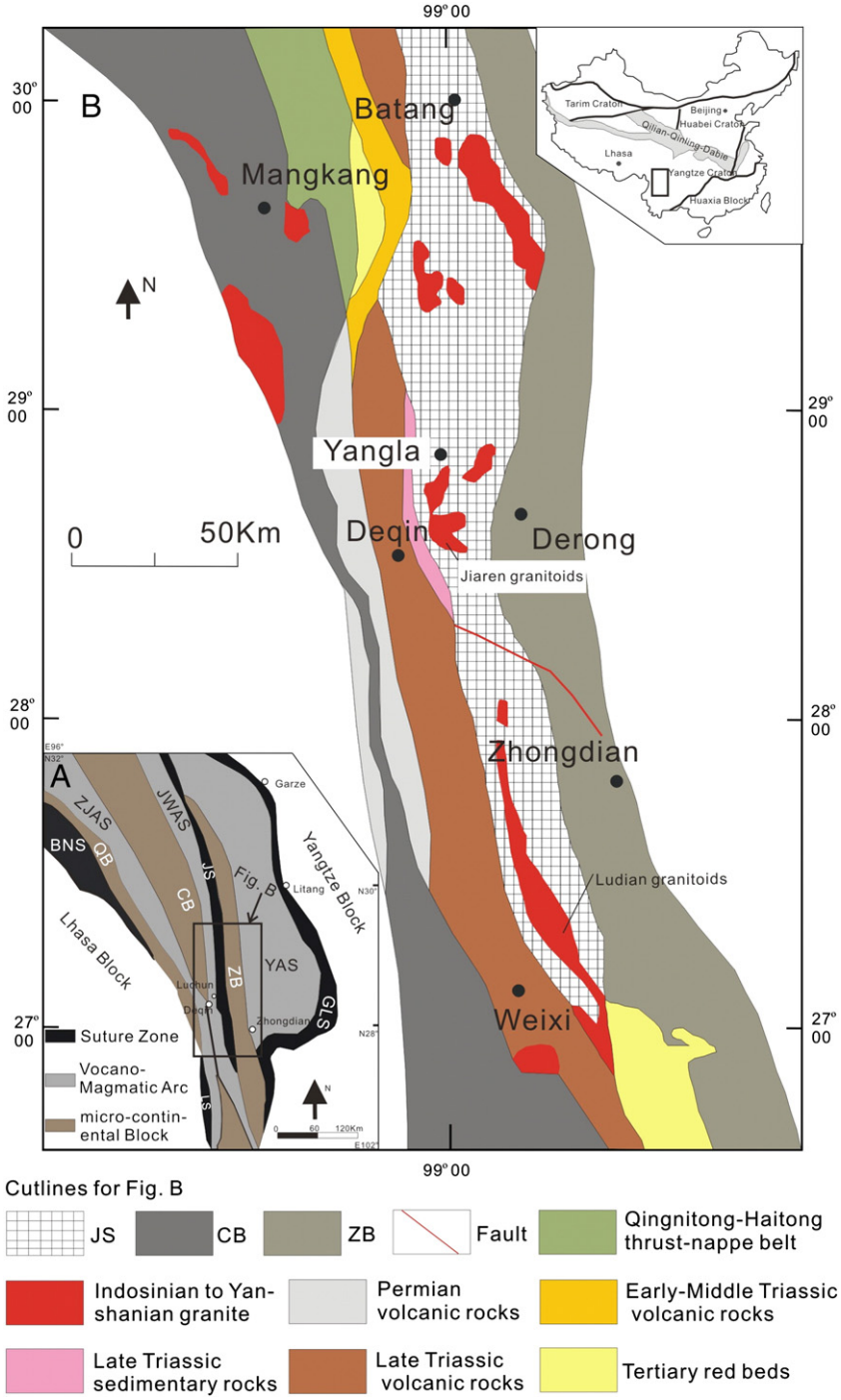

Fig. 1. Sketch showing tectonic framework (A) and the distribution of magmatic rocks (B) in the Jinshajiang suture zone and adjacent areas (modified after Hou et al. (2003)). Abbreviations: GLS = Garze–Litang Suture Zone; JS = Jinshajiang Suture Zone; LS = Lancangjiang Suture Zone; BNS = Bangonghu–Nujiang Suture Zone; YAS = Yidun Arc; JWAS = Jomda–Weixi Arc; ZJAS = Zaduo–Jinghong Arc; ZB = Zhongza micro-continental Block; CB = Changdu–Simao micro-continental Block; QB = Qiangtang micro-continental Block.

Changning–Menglian oceans from east to west (Mo et al., 1993; Mo and Pan, 2006; Jian et al., 2009a, 2009b; Pan et al., 2002, 2003; Fig. 1A). The birth and final closure of the Paleo-Tethys Ocean are associated with the breakup and assembly of Gondwanaland (Wang et al., 2000; Xiao et al., 2008). It has been commonly accepted that the Changning-Menglian Suture Zone is the main boundary that separates the Yangtze Block from Gondwanaland (Fan et al., 2009; Jian et al., 2009a, 2009b; Xiao et al., 2008), and that the Changdu-Simao and Zhongza micro-continental Blocks were marginal terranes of the Yangtze Block (Mo et al., 1993; Metcalfe, 2002; Wang et al., 2000; Fig. 1). In the SD, granites are widespread (Fig. 1B), among which the Indosinian (Triassic to Late Jurassic) granitoids have a large proportion (Hou et al., 2001; Lü et al., 1993; Peng et al., 2006; Reid et al., 2005, 2007; Roger et al., 2004; Wang et al., 1999, 2008; Xiao et al., 2007; Zhang et al., 2006, 2007, 2008a). Recently, the Indosinian granitoids in the Yidun Arc (Hou et al., 2001; Reid et al., 2005, 2007) and the Songpan–Garze belt (Roger et al., 2004; Xiao et al., 2007, Zhang et al., 2006, 2007, 2008a) have been thoroughly studied. However, the granites in the Jinshajiang suture zone have received little attention. Furthermore, a number of Indosinian ore deposits occur in this suture zone, such as the Yangla copper deposit (Zhan et al., 1998), Luchun–Hongpo Cu–Pb–Zn (Ag) polymetallic ore deposit (Wang et al., 2002) and Zhaokalong iron deposit (Hou et al., 2003, 2007), which are genetically associated with their host plutons. Obtaining accurate constraints on the nature and age of these granites has particular significance for our understanding of tectonic evolution and metallogeny of the Jinshajiang zone.

The Yangla copper deposit (Fig. 2), with prospective 1.3 Mt Cu reverses and an average copper grade of 1%, is located in the middle segment of the Jinshajiang Suture Zone (Zhan et al., 1998). In the mining district, the Beiwu, Linong and Lunong granitic intrusions, which are genetically associated with the deposit, exhibit a linear distribution in the south direction. Systematic studies for those intrusions are significant to understand the genesis of the deposit. Previous studies yielded a Rb–Sr whole-rock isochron age of 227 Ma for the Linong intrusions (Wei et al., 1997), and the Beiwu, Linong and Lunong granitoids were considered as the continental margin arc-type granite related to the subduction of the Jinshajiang Ocean to the Changdu–Simao micro-continental Block (Wei et al., 1997, 2000; Zhan et al., 1998). However, owing to the lack of isotopic data, the origin of granitoids and tectonic setting remain poorly understood. More precise ages also should be obtained. The Beiwu and Linong granitoids intruded into same sequences as the Linong intrusion, and the distance between each other is roughly 2 km, so both the Beiwu and Lunong granitoids have been analyzed. In this paper, we present the SIMS zircon U–Pb data, zircon oxygen isotopes, geochemical and Sr–Nd–Pb isotopic compositions of the three granitic intrusions from the Jinshajiang Suture Zone. The objectives of this study are (1) to elucidate the origin and petrogenesis of these granitoids; and (2) to determine the tectonic setting. We propose a model involving three-component mixing for the origin of granitoids.

2. Geological setting

The Jinshajiang Ocean is considered as a back-arc basin when the Changdu–Simao micro-continental Block split away from the Yangtze Block in Late Devonion or Early Carboniferous (Metcalfe, 2002; Mo et al., 1993; Wang et al., 2000). The Jinshajiang Suture Zone was formed after the closure of the Jinshajiang Ocean (Mo et al., 1993), bounded by the eastern Zongza micro-continental Block and the western Jamda–Weixi arc belt (Fig. 1). It is 20–40 km wide and over 1000 km long, extending from Eastern Tibet through Western Sichuan to Western Yunnan (Hou et al., 2003).

Such N–S trending area comprises four tectono-stratigraphic units, including the Eaqing Complex, the Jinshajiang Ophiolitic Melange, the Gajinxueshan Group and the Zhongxinrong Group (Xiao et al., 2008).

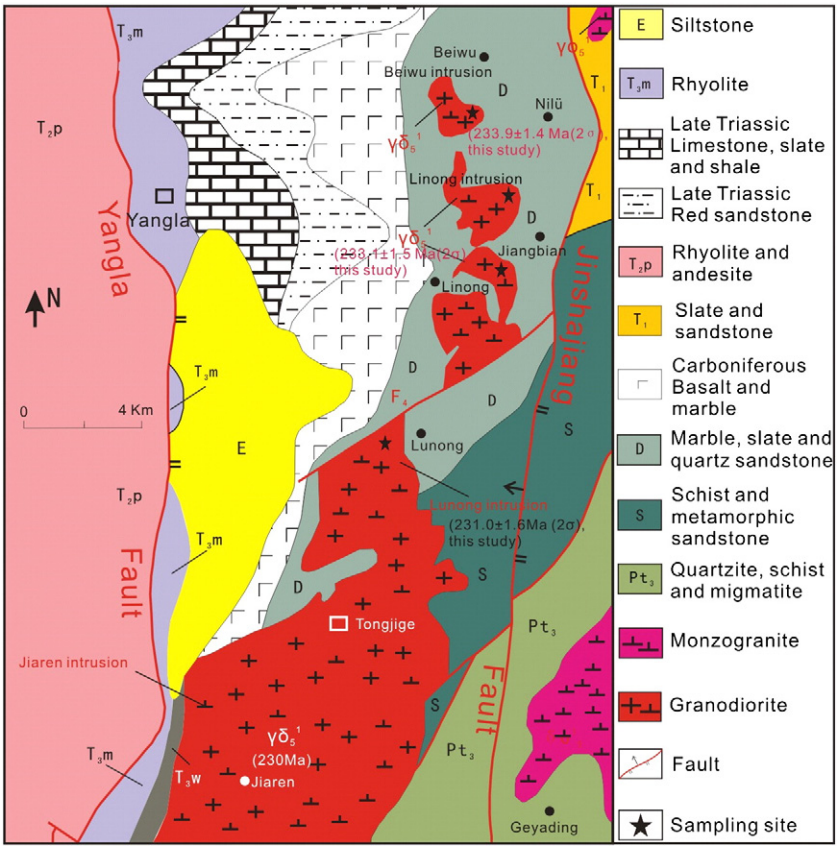

Fig. 2. Geological map of the Yangla copper deposit and the distribution of granitoids (modified after Zhu et al. (2009)).

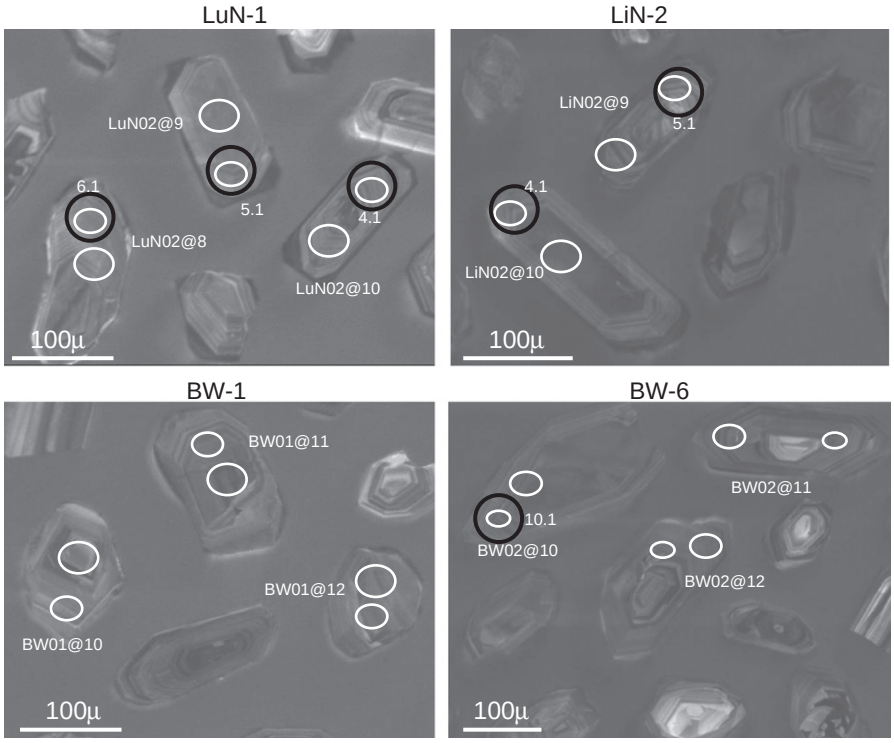

Fig. 3. CL images of representative zircons analyzed for *in situ* U–Pb and Hf–O isotopes. The big white ellipses indicate the SIMS analyzing spots for U–Pb, and the small white circles denote the analyzing spots for O isotopes. The black circles represent the analyzing spots for Hf isotopes. Numbers such as LuN02@9 are according to spot numbers in Appendix A and Appendix B, and numbers such as 4.1 are the same as spot numbers in Appendix C.

The Eaqing complex is composed of epidote–amphibolite facies to amphibolite facies metamorphic rocks. A zircon sample from the Eaqing complex gives an upper intercept U–Pb age of 1627 ± 192 Ma (Wang et al., 2000), indicating the presence of the Meso- to Neo-Proterozoic metamorphic basement in the Jinshajiang Suture Zone. The Jinshajiang Ophiolitic Melange comprises complex oceanic components. Two plagiogranites in the ophiolitic assemblage have zircon U–Pb ages of 340 ± 3 Ma and 294 ± 3 Ma (Wang et al., 2000), and the SHRIMP zircon U–Pb age of a cumulate gabbro from the Jinshajiang ophiolite is 343.5 ± 2.7 Ma (Jian et al., 2009b). These suggest that the opening and spreading of the Jinshajiang Ocean basin was mainly during the Carboniferous, but ranging from Early Carboniferous to Early Permian. Previous studies suggest that the Gajinxueshan Group was characterized by turbiditic clastic sediments, which has been previously interpreted as Permian in age by SBGMR (1997). Recent studies, however, reveal that the Group is composed of Late Devonian to Carboniferous carbonates, clastic sediments and basic volcanic rocks, and the age of these rocks may possibly extend into Permian (Zhu et al., 2009). The Zhongxinrong Group is in fault contact with the underlying Gajinxueshan Group. It is composed of flysch sediments and Upper Triassic molasse sequences. Granites intrude the flysch sequences and have Latest Permian–Triassic ages from 238 Ma to 255 Ma (Wang et al., 2000), which are interpreted to be generated under a syn-collisional setting. Combined with the existence of unconformity between the Yiwanshui Formation of Upper Triassic and underlying ophiolite (Mo and Pan, 2006), in Yuanjiang and Mojiang of western Yunnan, it is suggested that the collision was completed before Late Triassic.

In the suture zone, a series of Indosinian granitoids display a linear distribution from south to north, with total exposed area exceeding 1000 km^2 (Fig. 1B). Only a few studies have been reported about these granitic intrusions, i.e., the Ludian and Jiaren granitoids. The Ludian granitoids (~532 km^2; Fig. 1B) occur in the south of the suture zone, intruding the Cuiyibi Formation of Upper Triassic and underlain by the Shizhongshan Formation. They have zircon U–Pb ages of 239 ± 6 Ma (Jian et al., 2003). The Jiaren granitoids (~150 km^2; Fig. 1B) are located to the south of Yangla ore district, having a SIMS zircon U–Pb age of ca. 230 Ma (personal communication with Dr. Cheng-biao Leng, Institute of Geochemistry, Chinese Academy of Sciences, Guiyang). It has been suggested that these Indosinian granitoids in the area are genetically associated with the evolution of the Jinshajiang Ocean (Jian et al., 2003; Zhan et al., 1998).

3. Petrography and sampling

The Beiwu, Linong and Lunong granitoids refer to a narrow N–S trending area in the Yangla copper deposit, bounded by the Yangla Fault to the west and the Jinshajiang Fault to the east (Fig. 2). The Lunong intrusion is the northern part of the Jiaren granitoids (~150 km^2). They were all in fault contact with the overlying Silurian to Devonian sequences (Zhu et al., 2009), including marbles, metamorphic quartz sandstone, slates and schists. In the outer mining district, there occur large-scale Early Carboniferous basalts with interbedded marbles and Late Triassic sequences that are composed of rhyolites, red sandstones and limestones (Fig. 2; Zhan et al., 1998). The mineralization commonly occurs in the exo-contact zone of the intrusions, between the marble and sandstone sequences, and comprises skarn-type and quartz–sulphide ores. The ore bodies are made up of a series of tabular sheets or ore lens, and these ore lenses have various thicknesses from 2.2 to 64 m and extend over a 1600-m strike length (Hou et al., 2003). In general, the Yangla copper deposit is genetically related to the Beiwu, Linong and Lunong granitoids (Qu et al., 2004).

The Beiwu granitic intrusion in the northern part of the mining district, has an oval shape with an outcrop area of ca. 0.5 km^2. Principal rock types are medium-grained to coarse-grained granodiorite, consisting of 40% plagioclase, 15%–20% K-feldspar, 20%–25% quartz, 10%–15% hornblende and minor amount of biotite (<5%). Accessory minerals include zircon, apatite, magnetite and titanite. Twelve samples were collected throughout the Beiwu intrusion for

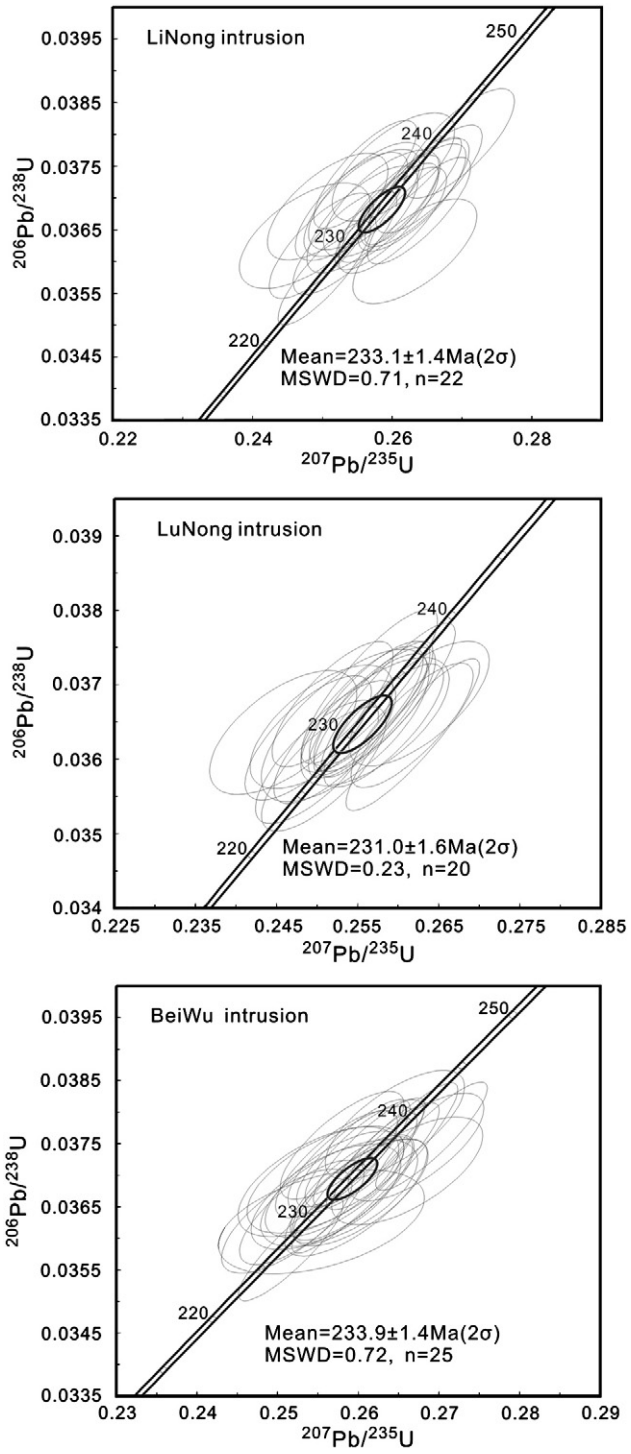

Fig. 4. U–Pb concordia diagram and weighted average $^{206}Pb/^{238}U$ ages for zircons from the Beiwu, Linong and Lunong granitoids.

analysis, among which samples BW-1 and BW-6 were collected for extracting zircons. The Linong granitic intrusion occurs in the middle part of the Yangla mining area, exhibiting an oval shape. It is about 2 km long and 1.5 km wide, with a total exposed area of 2.6 km^2. Rock types of the Linong intrusion include medium-grained to coarse-grained granodiorite in the core and monzogranite in the rim. The granodiorite is predominant, containing 35% plagioclase (An_{32-48}), 15%–20% K-feldspar, 20%–25% quartz, 10%–15% hornblende, minor amount of biotite (<5%), as well as accessory minerals including zircon, apatite, magnetite and titanite. The monzogranite is fine-grained to medium-grained, with more K-feldspar and less plagioclase (An_{23-32}) than the granodiorite. Thirteen samples have been collected from the Linong intrusion, and samples LiN-1 and LiN-2 were used for extracting zircons. The Lunong granitic pluton is to the south of the Linong intrusion, separated by F_4 fault (Fig. 2). Generally, the Lunong intrusion has similar petrological characteristics with the Beiwu granitoid pluton. Two zircon samples (LuN-1 and LuN-2) have been collected. All the granitic rocks show minor alteration with feldspar slight sericitization and silicification. It is necessary to note that there are lots of mafic microgranular enclaves (MMEs) in the Linong intrusion, which have a clear or blurry contact with the host rocks, with variable sizes (2–15 cm).

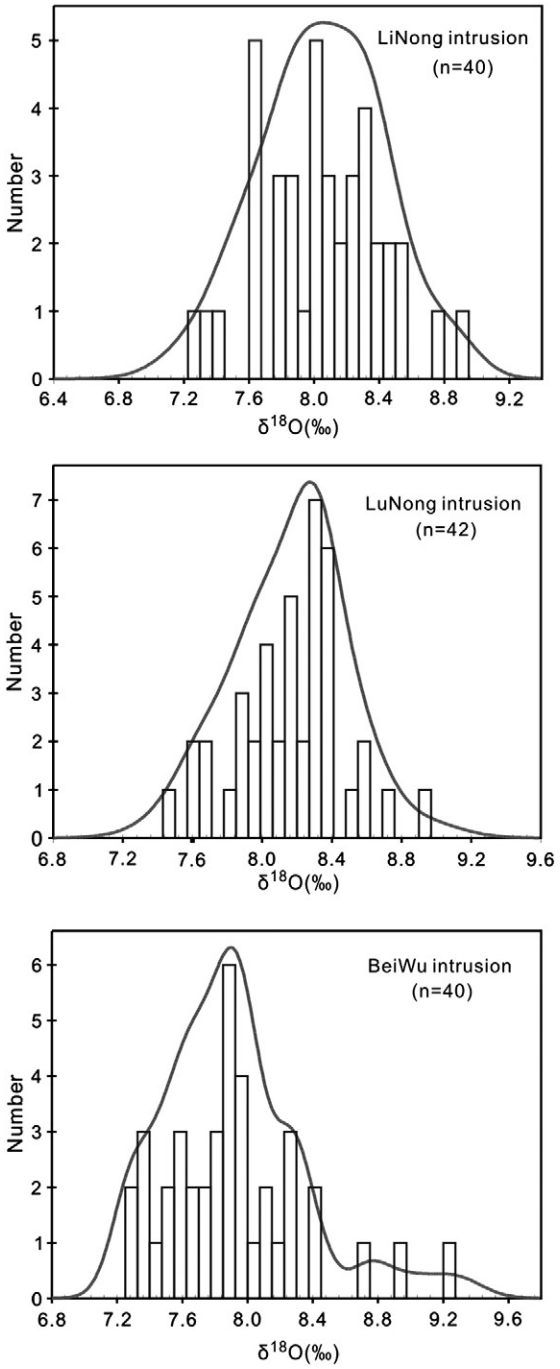

Fig. 5. Histogram of $\delta^{18}O$ values for the zircons from the Beiwu, Linong and Lunong granitoids.

Table 1
The analytical results of major (wt.%) and trace elements (ppm) of the Beiwu, Linong and Lunong intrusions.

The Linong intrusion													
Sample no.	LiN-1	LiN-2	LiN-3	LiN-4	LiN-5	LiN-6	LiN10-1	LiN10-2	LiN10-3	LiN10-4	LiN10-5	LiN10-6	LiN10-7
SiO_2	71.50	68.50	72.11	73.49	66.04	65.20	70.30	70.11	67.00	70.25	71.00	69.34	70.57
Al_2O_3	14.24	15.80	14.58	13.56	16.26	16.35	15.10	15.10	15.78	15.17	15.11	14.34	14.60
Fe_2O_{3T}	2.83	2.25	2.16	1.93	3.19	4.39	2.90	2.91	4.19	2.65	2.58	3.68	2.60
CaO	2.41	4.03	2.34	1.90	5.21	4.16	2.86	2.66	3.76	2.85	2.72	3.49	2.50
MgO	0.84	1.58	0.65	0.52	1.76	1.81	0.79	0.89	1.26	0.77	0.71	1.17	0.74
Na_2O	2.77	3.93	2.97	2.72	3.52	2.87	3.24	3.13	3.05	2.98	3.12	2.69	2.95
K_2O	3.94	1.89	4.05	4.29	2.15	2.99	3.41	3.71	3.25	3.90	3.64	3.40	3.76
TiO_2	0.28	0.39	0.19	0.17	0.47	0.45	0.24	0.26	0.35	0.26	0.24	0.30	0.23
MnO	0.05	0.03	0.03	0.04	0.05	0.06	0.02	0.03	0.07	0.03	0.04	0.05	0.02
P_2O_5	0.063	0.096	0.051	0.041	0.111	0.113	0.082	0.086	0.092	0.083	0.083	0.074	0.08
LOI	0.75	1.19	0.66	0.9	0.92	1.12	1.04	1	0.93	0.85	0.72	1.53	1.18
Total	99.66	99.69	99.8	99.56	99.67	99.52	100	99.9	99.74	99.8	99.96	100.05	99.24
Ga	–	16.2	13.2	12.5	14.9	17.7	17.2	17.5	17.0	17.3	17.3	15.1	17.0
Rb	–	73.1	181	167	73.6	112	145	156	127	160	164	143	149
Sr	–	491	167	146	297	329	287	249	305	255	232	256	242
Zr	–	86.6	90.2	91.2	104	91.6	115	114	130	121	110	113	114
Nb	–	9.86	7.14	7.78	11.80	10.80	9.50	10.70	9.20	9.70	9.60	6.90	9.70
Ba	–	280	551	616	434	771	679	613	644	613	598	609	578
Hf	–	2.35	2.66	2.88	2.97	2.45	3.50	3.50	3.60	3.70	3.40	3.30	3.60
Ta	–	0.885	0.972	1.27	1.15	0.81	1.20	1.50	1.00	1.30	1.20	0.9	1.4
Pb	–	19.8	33.5	34.0	28.8	28.4	30.0	32.0	22.0	36.0	35.0	29.0	38.0
U	–	4.99	4.96	4.27	3.46	2.57	4.25	3.91	3.18	3.92	3.21	3.22	3.94
Th	–	22.9	23.0	20.2	13.9	15.4	16.8	15.8	16.7	16.0	14.3	22.1	15.3
La	–	25.7	28.1	25.9	21.1	19.0	22.3	25.8	28.9	26.6	24.9	24.4	26.2
Ce	–	57.0	59.4	53.5	49.3	45.2	40.3	46.7	50.1	48.8	45.9	42.7	48.4
Pr	–	5.07	4.70	4.52	4.86	4.39	4.23	4.89	5.03	5.19	4.77	4.23	5.08
Nd	–	17.8	14.6	14.3	18.5	16.7	14.6	16.4	16.8	18.1	16.8	14.3	17.2
Sm	–	3.15	2.66	2.32	3.69	3.23	2.85	3.14	2.88	3.41	3.30	2.60	3.48
Eu	–	0.822	0.557	0.522	0.760	0.967	0.730	0.700	0.820	0.740	0.760	0.700	0.730
Gd	–	2.72	2.41	1.99	3.30	3.03	2.70	2.81	2.77	3.10	2.98	2.42	3.22
Tb	–	0.344	0.320	0.270	0.491	0.434	0.380	0.380	0.390	0.430	0.390	0.340	0.450
Dy	–	2.09	2.07	1.74	3.18	2.69	1.92	1.91	2.06	2.13	1.94	1.97	2.19
Ho	–	0.418	0.404	0.335	0.606	0.548	0.350	0.350	0.410	0.400	0.350	0.380	0.410
Er	–	1.13	1.34	1.05	1.73	1.64	1.05	1.05	1.31	1.17	1.06	1.25	1.19
Tm	–	0.165	0.202	0.165	0.258	0.227	0.140	0.160	0.190	0.150	0.150	0.180	0.170
Yb	–	1.13	1.55	1.30	1.91	1.48	1.01	1.02	1.31	1.06	0.99	1.23	1.18
Lu	–	0.163	0.221	0.204	0.281	0.220	0.150	0.160	0.220	0.170	0.150	0.190	0.180
Y	–	12.9	13.5	11.8	20.2	16.6	10.3	10.8	11.9	11.4	10.6	10.9	12.2

The Lunong intrusion												
Sample no.	LuN-1	LuN-2	LuN-3	LuN-4	LuN-5	LuN10-1	LuN10-2	LuN10-3	LuN10-4	LuN10-6	LuN10-7	LuN10-8
SiO_2	67.00	66.03	66.90	69.00	66.73	67.50	67.86	68.03	68.16	66.79	67.00	68.10
Al_2O_3	16.03	16.02	15.99	14.65	15.59	15.14	14.83	14.89	15.21	15.60	15.48	15.27
Fe_2O_{3T}	3.15	3.99	3.40	3.65	4.02	2.98	3.87	3.71	2.09	2.73	2.06	3.06
CaO	3.61	3.62	3.61	3.27	3.57	4.02	3.21	4.10	5.24	3.97	4.43	3.08
MgO	1.64	1.58	1.37	1.32	1.48	1.39	1.24	1.30	1.19	1.54	1.23	1.25
Na_2O	3.03	2.92	3.16	2.78	3.01	3.08	2.70	3.08	3.24	4.22	3.28	3.18
K_2O	3.62	3.69	3.82	3.57	3.70	3.81	3.84	3.16	3.26	3.20	4.36	3.69
TiO_2	0.41	0.40	0.35	0.34	0.39	0.36	0.33	0.35	0.36	0.35	0.39	0.30
MnO	0.05	0.07	0.05	0.05	0.06	0.05	0.06	0.05	0.03	0.05	0.04	0.04
P_2O_5	0.101	0.101	0.087	0.086	0.096	0.09	0.08	0.088	0.088	0.087	0.095	0.074
LOI	1.15	1.21	1.24	1.16	1.24	1.28	1.25	1.35	0.75	1.4	1.21	1.95
Total	99.8	99.62	100	99.89	99.89	99.71	99.28	100.11	99.63	99.98	99.59	100
Ga	17.6	15.8	18.0	16.0	17.7	15.9	16.0	17.0	15.4	16.0	15.7	15.6
Rb	120	138	152	145	154	130	152	113	102	121	149	128
Sr	413	286	320	274	300	338	318	277	296	378	374	248
Zr	91.1	75.8	130	114	124	134	128	150	140	146	119	115
Nb	9.00	9.45	9.00	8.90	9.70	8.30	7.60	8.50	8.30	8.10	9.00	7.00
Ba	674	644	665	598	677	655	694	532	484	674	600	634
Hf	2.58	2.15	4.10	3.60	3.90	3.90	3.70	4.40	4.00	4.40	3.50	3.40
Ta	0.899	0.912	1.1	1.00	1.20	1.10	0.9	1.20	1.10	1.10	1.10	1.10
Pb	32.3	29.7	42.0	36.0	39.0	38.0	25.0	28.0	31.0	34.0	32.0	25.0
U	2.79	4.50	4.33	7.37	5.65	3.20	1.92	3.19	3.74	4.01	3.44	2.44
Th	25.6	35.8	28.4	65.2	34.9	17.0	14.7	42.3	20.3	21.7	16.9	16.6
La	64.5	48.9	25.3	25.6	33.9	28.4	24.5	101.0	34.6	36.3	30.4	24.1
Ce	96.3	98.0	45.3	45.8	58.5	49.4	42.6	155.5	56.5	62.0	51.1	42.0
Pr	9.26	8.59	4.77	4.80	5.94	5.05	4.34	13.80	5.54	6.04	5.13	4.31
Nd	28.2	28.2	16.3	16.1	20.0	16.4	14.8	39.5	17.8	19.7	17.1	14.3
Sm	3.95	4.31	2.85	2.88	3.43	2.96	2.59	5.01	3.00	3.14	3.03	2.59
Eu	0.964	0.825	0.790	0.730	0.780	0.710	0.700	0.860	0.750	0.720	0.760	0.660
Gd	3.23	3.68	2.78	2.85	3.21	2.94	2.57	4.93	3.08	3.04	2.94	2.45
Tb	0.430	0.448	0.410	0.400	0.440	0.430	0.390	0.550	0.420	0.410	0.430	0.360

(continued on next page)

Table 1 (*continued*)

The Linong intrusion													
Sample no.	LiN-1	LiN-2	LiN-3	LiN-4	LiN-5	LiN-6	LiN10-1	LiN10-2	LiN10-3	LiN10-4	LiN10-5	LiN10-6	LiN10-7
Dy		2.54	2.63	2.31	2.27	2.51	2.34	1.95	2.74	2.30	2.18	2.46	1.97
Ho		0.498	0.527	0.470	0.470	0.490	0.460	0.400	0.530	0.490	0.450	0.500	0.410
Er		1.53	1.54	1.47	1.38	1.46	1.49	1.34	1.77	1.53	1.46	1.58	1.27
Tm		0.211	0.196	0.210	0.220	0.220	0.220	0.190	0.250	0.220	0.230	0.220	0.200
Yb		1.46	1.42	1.52	1.43	1.53	1.51	1.37	1.79	1.50	1.59	1.58	1.40
Lu		0.229	0.215	0.250	0.240	0.250	0.260	0.210	0.290	0.250	0.270	0.240	0.230
Y		16.3	16.4	13.5	12.8	14.6	13.8	12.1	15.8	13.9	13.4	14.4	12.2

The Beiwu intrusion												
Sample no.	BW-1	BW-2	BW-3	BW-4	BW-5	BW-6	BW10-1	BW10-2	BW10-3	BW10-4	BW10-5	BW10-6
SiO_2	65.65	65.71	66.50	65.00	64.53	67.00	66.00	65.47	65.91	65.00	66.75	66.88
Al_2O_3	14.87	15.56	15.39	15.73	15.98	14.87	15.39	15.46	15.84	15.41	15.12	14.90
Fe_2O_{3T}	3.88	3.42	3.78	4.17	4.19	3.59	4.05	4.04	3.77	4.42	3.72	4.41
CaO	2.90	2.92	1.95	2.41	2.78	2.37	3.27	2.85	3.10	2.63	2.52	1.89
MgO	1.48	1.37	1.51	1.61	1.55	1.43	1.30	1.37	1.23	1.41	1.24	1.39
Na_2O	3.01	4.65	3.66	3.61	3.78	3.59	3.50	3.51	3.63	4.25	3.31	3.30
K_2O	3.44	2.87	3.52	3.58	3.28	3.52	3.10	3.65	3.36	3.10	3.79	3.91
TiO_2	0.41	0.38	0.38	0.42	0.43	0.36	0.35	0.34	0.34	0.41	0.38	0.38
MnO	0.05	0.04	0.06	0.06	0.06	0.06	0.05	0.07	0.06	0.05	0.04	0.05
P_2O_5	0.098	0.096	0.097	0.101	0.102	0.094	0.09	0.088	0.083	0.097	0.082	0.093
LOI	3.4	2.93	2.99	3.03	2.76	2.96	2.83	2.98	2.66	3.32	2.29	2.69
Total	99.18	99.93	99.83	99.72	99.44	99.83	99.94	99.84	100	100.1	99.25	99.91
Ga	15.4	15.1	16.0	15.4	14.2	14.7	16.6	16.9	16.9	16.8	16.4	17.1
Rb	145	112	123	139	103	130	114	150	135	112	147	130
Sr	194	174	190	279	234	182	332	240	325	245	329	282
Zr	90.8	104	119	91.1	104	111	124	118	123	127	118	145
Nb	7.94	8.42	9.97	8.15	8.23	8.19	7.00	7.10	7.00	7.40	7.00	7.60
Ba	759	513	783	690	609	624	648	637	595	622	686	999
Hf	2.48	2.84	3.22	2.61	2.76	2.90	3.60	3.60	3.60	3.70	3.50	4.10
Ta	0.807	0.888	0.943	0.769	0.791	0.789	0.900	0.900	0.900	0.900	0.900	0.900
Pb	20.1	79.0	15.2	13.0	22.4	23.6	19.0	21.0	18.0	14.0	18.0	31.0
U	4.35	4.56	9.32	4.20	4.34	4.28	4.42	4.64	4.93	4.56	4.38	4.35
Th	15.0	15.8	16.8	13.0	13.8	13.0	16.4	18.0	17.8	15.3	18.2	16.0
La	21.7	23.1	27.5	21.7	27.1	21.4	27.3	32.0	30.4	25.3	34.0	30.8
Ce	49.0	51.8	56.8	49.1	62.6	47.2	47.9	55.4	53.9	45.3	59.2	55.4
Pr	4.40	4.61	5.17	4.50	5.55	4.39	4.93	5.52	5.45	4.85	5.89	5.78
Nd	14.6	15.4	17.0	15.2	19.4	15.9	16.6	18.1	17.9	16.6	19.0	20.0
Sm	2.56	2.80	3.22	2.72	3.43	3.02	2.96	3.14	2.98	3.21	3.11	3.73
Eu	0.655	0.713	0.845	0.680	0.813	0.849	0.750	0.780	0.760	0.750	0.760	0.810
Gd	2.30	2.61	2.94	2.57	3.09	2.69	2.79	3.00	3.09	3.24	3.15	3.57
Tb	0.329	0.364	0.390	0.381	0.445	0.360	0.410	0.420	0.430	0.460	0.410	0.510
Dy	2.08	2.29	2.38	2.40	2.59	2.30	2.20	2.41	2.29	2.71	2.25	2.73
Ho	0.419	0.442	0.500	0.488	0.516	0.463	0.450	0.470	0.470	0.550	0.460	0.550
Er	1.17	1.31	1.47	1.34	1.46	1.28	1.47	1.49	1.49	1.75	1.48	1.65
Tm	0.186	0.189	0.207	0.200	0.217	0.199	0.210	0.220	0.230	0.260	0.210	0.250
Yb	1.27	1.31	1.48	1.44	1.57	1.40	1.48	1.51	1.54	1.72	1.54	1.57
Lu	0.194	0.220	0.217	0.214	0.245	0.210	0.230	0.250	0.250	0.280	0.260	0.260
Y	13.6	14.3	16.7	15.1	16.2	14.7	13.3	13.7	13.5	15.6	13.5	15.9

4. Analytical methods

Samples from the Beiwu (BW-1 and BW-6), Linong (LiN-1 and LiN-2) and Lunong (LuN-1 and LuN-2) granitoid plutons were collected for separating zircons using conventional heavy liquid and magnetic techniques. More than 1000 zircon grains have been recovered. Representative zircon grains were handpicked under a binocular microscope and mounted in an epoxy resin disc, and then polished and coated with gold film, which were documented with transmitted and reflected light micrographs as well as cathodoluminescence (CL) images to reveal their internal structures. The CL images were obtained using LEO1450VP scanning electron microscope at the Institute of Geology and Geophysics, Chinese Academy of Sciences, Beijing. The zircon U–Pb isotopic analyses and U, Th and Pb concentrations were also determined in the Institute of Geology and Geophysics, Chinese Academy of Sciences, Beijing, using the Cameca IMS-1280 SIMS. The analytical procedures are the same as those described by Li et al. (2009b). Measured compositions were corrected for common Pb using the measured non-radiogenic ^{204}Pb. Uncertainties on individual analyses are reported at 1σ level, and weighted mean ages for pooled U–Pb analyses are quoted with 95% confidence interval. Data reduction was carried out using the Isoplot program of Ludwig (2001).

Zircon oxygen isotopes were also measured using the Cameca IMS-1280 SIMS at the Institute of Geology and Geophysics. The detailed analytical procedures were described by Li et al. (2009a). The Cs^+ primary ion beam was used as the ion source, and the spot size is about 20 μm in diameter. Oxygen isotopes were measured using the multi-collection model on two off-axis Faraday cups. One analysis takes ca. 5 min. Uncertainties on individual analyses are usually better than 0.2‰–0.3‰ (1σ). The instrumental mass fractionation factor is corrected using zircon 91500 standards with a $\delta^{18}O$ value of 9.9‰ (Li et al., 2009a).

In situ zircon Hf isotopic analysis was carried out on a Nu plasma multi-collector ICPMS equipped with a UP-213 laser-ablation system (LA–MC -ICPMS) at the Institute of Geochemistry, Chinese Academy of Sciences. Most Lu–Hf isotopic measurements were made on the same zircon grains previously analyzed for U–Pb and O isotopes. During the course of this study, a laser repetition rate of 10 Hz was used and beam diameters were 60 μm. Laser beam energy density was 5.27–6.15 J/cm^2. The detailed analytical procedures were similar to those described by Tang et al. (2008). Our determined $^{176}Hf/^{177}Hf$ ratios of

0.282303 ± 0.000026 (2σ, n = 16) for zircon standards 91500 are in good agreement with the reported values (Woodhead et al., 2004).

Major elements of bulk rocks were determined on the Axios PW4400 X-ray fluorescence spectrometer (XRF) at the State Key Laboratory of Ore Deposit Geochemistry (SKLODG), Institute of Geochemistry, Chinese Academy of Sciences, using fused lithium–tetraborate glass pellets. The analytical precision is better than 5%. Trace elements were analyzed using a PE DRC-e ICP-MS at the SKLODG, with Rh being used as an internal standard to monitor signal drift during counting. The analytical uncertainty is usually less than 5%. The detailed analytical methods were introduced by Qi et al. (2000).

Whole-rock Sr–Nd–Pb isotopic compositions were obtained using a Finnigan Triton multi-collector mass spectrometer at China University of Geosciences, Wuhan. The mass fractionation corrections for Sr and Nd isotopic ratios are based on $^{86}Sr/^{88}Sr = 0.1194$ and $^{146}Nd/^{144}Nd = 0.7219$, respectively. The $^{87}Sr/^{86}Sr$ ratios of the NBS987 Sr standards and $^{143}Nd/^{144}Nd$ ratios of the La Jolla Nd standards determined during this study were 0.710254 ± 0.000008 (n = 18) and 0.511856 ± 0.000012 (n = 15) respectively. Total procedural Sr and Nd blanks are $Rb = 3\times10^{-11}$, $Sr = 1.2\times10^{-10}$; $Sm = 3\times10^{-11}$, and $Nd = 1.2\times10^{-10}$, respectively. Details were given by Zhou et al. (2007). Pb was separated by a conventional AG50 1×8 anion exchange technique. The $^{206}Pb/^{204}Pb$, $^{207}Pb/^{204}Pb$ and $^{208}Pb/^{204}Pb$ ratios of the NBS981 Pb standards were 16.932, 15.485 and 36.685, respectively. The analytical procedures are the same as those described by Liu et al. (2001).

5. Results

5.1. SIMS zircon U–Pb ages

SIMS zircon U–Pb data are listed in Appendix A, and representative zircon CL images and spot analyses are shown in Fig. 3, where the analytical spots are pointed by the bigger ellipses. Most zircons from Beiwu, Linong and Lunong intrusions are dominated by light pink to colorless euhedral crystals, and a minor component are grainy. They have euhedral shape and range from 100 to 350 μm in length, with length to width ratios from 2:1 to 3:1. There's good oscillatory zoning, indicative of magma zircons (Fig. 3). For those three intrusions, thirty analyses of 30 zircon samples were obtained in sets of five scans during a single analytical session.

Zircons of the Beiwu granodioritic intrusion (Appendix A) have highly variable U (239–1696 ppm) and Th (65–634 ppm), with variable Th/U ratios (0.103–0.701). Common Pb is variable, with f_{206} values, the proportion of common ^{206}Pb in total measured ^{206}Pb being 0.00–21.49%. The higher f_{206} may be related to fractures in the zircons, possibly due to the atmosphere during making discs. Zircons with higher f_{206} have discordant ages of $^{206}Pb/^{238}U$ and $^{207}Pb/^{235}U$. The remaining 25 spot analyses with lower f_{206} yielded a concordant age of 233.9 ± 1.4 Ma (2σ), and they have $^{206}Pb/^{238}U$ ages ranging from 226.9 to 236.5 Ma (Fig. 4), giving a weighted mean age of 233.9 ± 1.4 Ma (2σ, MSWD = 0.72, with 95% confidence interval), which is similar to the concordant age. It is interpreted as the magma crystallization age of the Beiwu intrusion.

Zircons from the Linong granitoid intrusion (Appendix A) have high U (429–1561 ppm) and variable Th (101–1024 ppm), with Th/U ratios of 0.229–0.615. The remaining 22 spot analyses have lower f_{206} (<0.5%) and yielded a concordant age of 233.0 ± 1.5 Ma (2σ). In addition, they have $^{206}Pb/^{238}U$ ages ranging from 226.9 to 237.2 Ma (Fig. 4), giving a weighted mean age of 233.1 ± 1.4 Ma (2σ, MSWD = 0.71, with 95% confidence interval). It is interpreted as the best estimate of crystallization age for the Linong intrusion.

Zircons from the Lunong granodioritic intrusion (Appendix A) are similar with the above two intrusions. They also have variable concentrations of U (665–1443 ppm) and Th (169–700 ppm), with lower Th/U ratios (0.241–0.564 ppm). Spot LuN01@14 (Appendix A) has relatively lower $^{206}Pb/^{238}U$ ages, resulting from the loss of Pb. The remaining 20 spot analyses with lower f_{206} (<0.5%) yielded a concordant age of 231.0 ± 1.6 Ma (2σ). They have $^{206}Pb/^{238}U$ ages ranging from 227.2 to 234.1 Ma (Fig. 4), giving the same weighted mean age (2σ, MSWD = 0.23, with 95% confidence interval). It is interpreted as the magma crystallization age of the Lunong intrusion. The Beiwu, Linong and Lunong intrusions have similar ages within the uncertainty, indicating the derivation from the same magmatic event.

5.2. Zircon O isotopes

Forty O isotopic analyses were conducted on zircons from the above intrusions (including 30 zircons measured for U–Pb dating). The data are presented in Appendix B. Zircons from the Beiwu intrusion exhibit a relatively wide range of oxygen isotopic compositions ($\delta^{18}O = 7.3‰–9.3‰$), which form a normal Gaussian distribution (Fig. 5) with an average of $\delta^{18}O = 7.9‰$. Zircons from the Linong intrusion have relatively homogenous oxygen isotopic compositions: 7.4‰–8.9‰, showing a normal distribution with an average of 8.1‰. The Lunong intrusion also has a homogenous $\delta^{18}O$ (7.6‰–8.9‰), and the average ratio is 8.1‰. The similar oxygen isotopic compositions of the three intrusions suggest they may have a common source region.

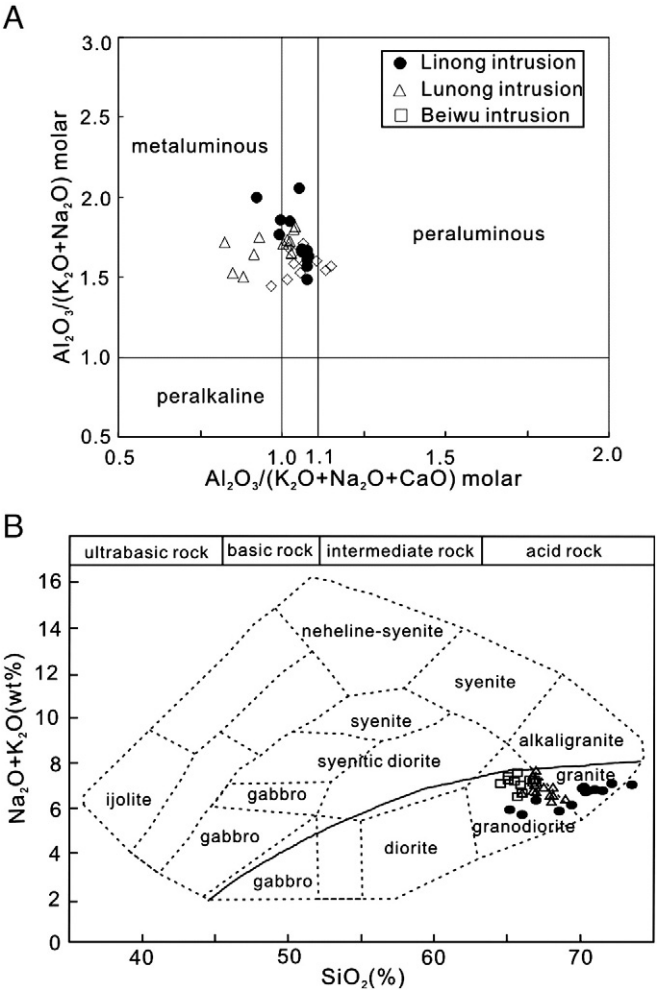

Fig. 6. (A) Whole-rock SiO_2 vs. $(K_2O + Na_2O)$ classification diagram of the Beiwu, Linong and Lunong plutons (Middlemost, 1994); (B) chemical composition of the Beiwu, Linong and Lunong granitoids in terms of alumina saturation.

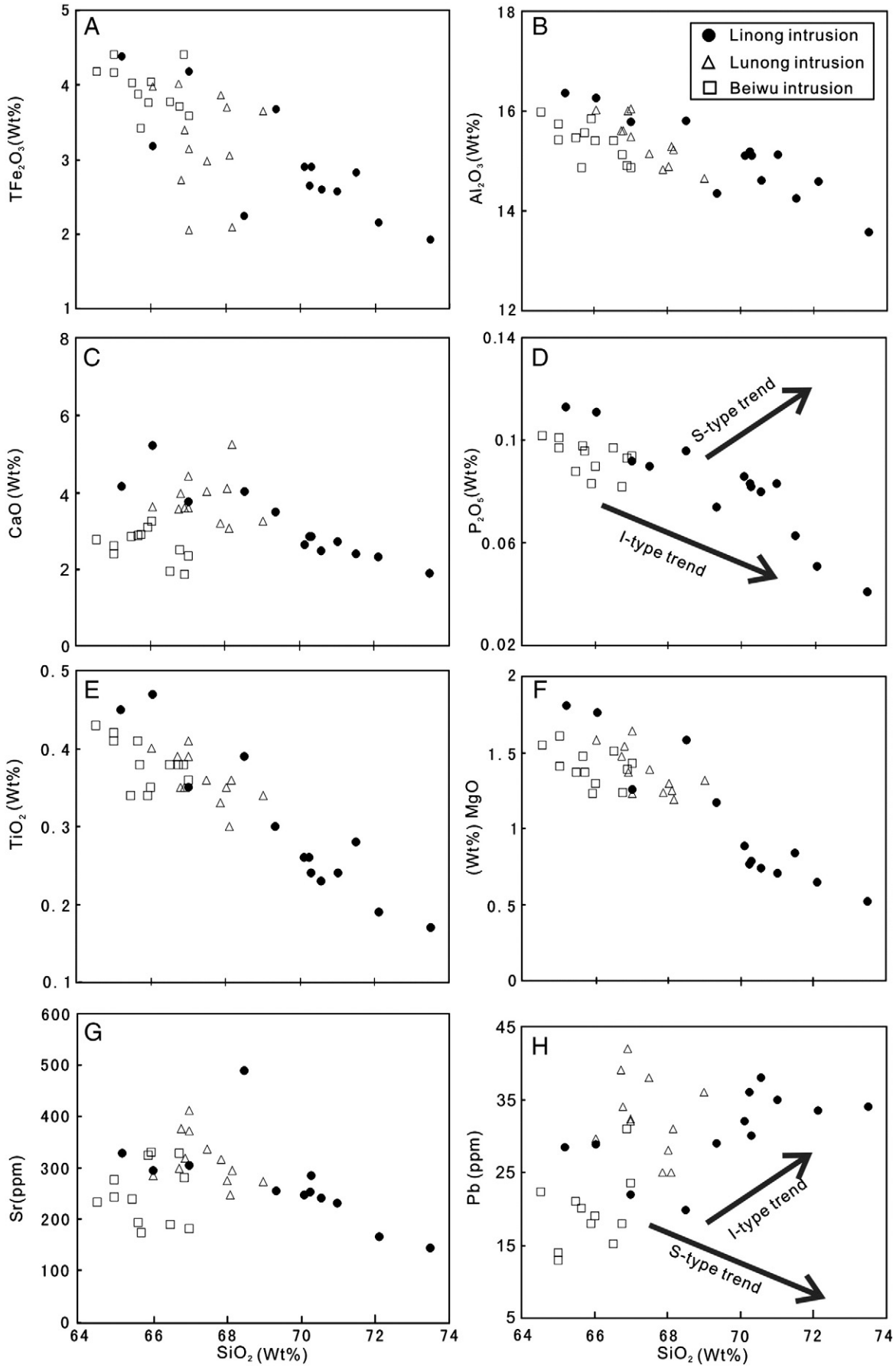

Fig. 7. Selected variation diagrams of major element oxides and silica for the Beiwu, Linong and Lunong granitoids. I-type granite trend is after Chappell and White (1992) and Chappell (1999).

5.3. Zircon Hf isotopes

Three samples (BW-6, LiN-2 and LuN-2) of zircons dated by U–Pb and measured for oxygen isotopes were mostly analyzed for their Lu–Hf isotopes on the same grains (Fig. 3), and the results are listed in Appendix C. The $\varepsilon_{Hf}(t)$ values and two-stages model ages (T_{DM2}) were calculated at 230 Ma. Ten spot analyses were obtained for sample (BW-6) from the Beiwu intrusion, yielding $\varepsilon_{Hf}(t)$ values between lu.1 and +2.8 with T_{DM2} model ages of 1083 to 1453 Ma. Zircons from the Linong intrusion (LiN-2) have negative $\varepsilon_{Hf}(t)$ values of) .6 to −2.3 with T_{DM2} model ages of 1404–1800 Ma. Ten spot analyses from the Lunong intrusion (LuN-2) gave relatively homogeneous $\varepsilon_{Hf}(t)$ values and two-stage Hf model ages (1301–1518 Ma).

5.4. Major and trace elements

Major and trace elemental compositions for the rocks from the Beiwu, Linong and Lunong granitic intrusions are listed in Table 1. Rocks from the Linong pluton have a relatively wider range of SiO_2 (65.2–73.5 wt.%) than the Beiwu (64.5–66.9 wt.%) and Lunong (66.0–67.9 wt.%) granodioritite. Furthermore, the Linong granitoids have relatively high Na_2O (2.77–3.93 wt.%) and K_2O (1.89–4.29 wt.%), with high total alkali concentrations ($K_2O + Na_2O = 5.82–7.02$ wt.%) and K_2O/Na_2O ratios (0.48–1.58), medium contents of CaO (1.90–5.21 wt.%) and low Fe_2O_3 (total Fe) (1.93–4.19 wt.%), MgO (0.74–1.81 wt.%), TiO_2 (0.17–0.39 wt.%), MnO (0.02–0.07 wt.%) and P_2O_5 (0.06–0.11 wt.%). Al_2O_3 contents range from 13.6 to 16.4 wt.%. In general, the Lunong intrusion has similar major elemental compositions to the Linong granitoids. The Beiwu intrusion displays a narrow range of Na_2O (3.01–4.65 wt.%), K_2O (2.87–4.36 wt.%), Al_2O_3 (14.9–16.0 wt.%), CaO (1.89–3.27 wt.%), Fe_2O_3 (total Fe) (3.42–4.42 wt.%), MgO (1.24–1.61 wt.%), TiO_2 (0.34–0.43 wt.%), MnO (0.04–0.07) and P_2O_5 (0.08–0.10). Total alkali concentrations range from 6.45 wt.% to 7.52 wt.%, with $K_2O/Na_2O = 0.62–1.18$. In the plots of SiO_2–($K_2O + Na_2O$), they belong to granodiorite except for 7 samples from the Linong intrusion (Fig. 6B). Those 7 samples belong to monzogranite. A/CNK values [molar $Al_2O_3/(CaO + Na_2O + K_2O)$] range from 0.92 to 1.08 for the Linong intrusion, from 0.83 to 1.04 for the Lunong intrusion and from 0.97 to 1.15 for the Beiwu intrusion (Fig. 6A). They are dominantly metaluminous and slightly peraluminous. The variations of representative major elements are plotted against SiO_2 contents in the three intrusions (Fig. 7). With increasing silica, MgO, Fe_2O_3 (total Fe), Al_2O_3, TiO_2, P_2O_5 and MnO decreased, and CaO increased in the early-stage but decreased in the later. The three intrusions all have a large variation of trace elemental content (Table 1). The Beiwu granodiorites have 103–150 ppm Rb, 174–329 ppm Sr, 7.00–10.0 ppm Nb, 13.3–16.7 ppm Y and 0.77–0.90 ppm Ta. Comparatively, rocks from the Linong intrusion span wider ranges of Rb (73–181 ppm), Sr (146–491 ppm), Nb (6.9–11.8 ppm), Y (10.3–20.2 ppm) and Ta (0.86–1.50 ppm). The Lunong granodiorites have 102–154 ppm Rb, 242–413 ppm Sr, 7.00–9.70 ppm Nb, 12.1–16.4 ppm Y and 0.90–1.40 ppm Ta. Sr contents are plotted against SiO_2 in Fig. 7. It increases in the early stage and decreases in the later stage with increasing SiO_2 content. In primitive mantle-normalized spidergrams (Fig. 8A), all the samples exhibit similar trace elemental patterns, with significant negative anomalies of high field strength elements (HFSE, e.g., Nb, Ta, Ti, Zr and Hf) and P. There are positive anomalies of large-ion lithophile elements (LILE, e.g., Rb, Th, Ba and U). In addition, compared to Rb and Th, Ba has significantly negative anomalies.

The Beiwu, Linong and Lunong granitoids have similar chondrite-normalized REE profiles (Fig. 8B), and all have high total REE contents (92.7–328 ppm), with moderate to strong enrichment of light REE [$(La/Yb)_N = 7.92–40.3$] and a relatively flat heavy REE profile [$(Gd/Yb)_N = 1.26–2.49$]. All of the rocks have weak negative Eu anomalies, with Eu/Eu^* of 0.65 to 0.93. The high $(La/Yb)_N$ ratios and low Yb_N values (5.82–11.2) of all the intrusions suggest that the garnet was involvement in the genesis of their magma source.

These intrusions have 10,000 Ga/Al ratios ranging from 1.7 to 2.2 and FeO_T/MgO from 1.3 to 3.3, lower than typical A-type granites. In the plots (Fig. 9) of 10,000 Ga/Al vs. $K_2O + Na_2O$ and Zr (Whalen et al., 1987), both the samples fall in the fields of I- and S-type granites. These intrusions have low P_2O_5 (0.06–0.11) contents that are negatively correlated with SiO_2 (Fig. 7D). The features are consistent with the differentiation trend of I-type granites (Chappell, 1999; Li et al., 2007). Similarly, Pb contents (except BW-2) increase with increasing silica contents (Fig. 7H), indicating the evolutive trend of I-type granites (Chappell and White, 1992; Wu et al., 2003). Combined with normative corundum <1% and rare muscovite and cordierite, the Beiwu, Linong and Lunong intrusions belong to I-type granites.

5.5. Sr–Nd–Pb isotopes

Sr and Nd isotopic compositions of the Beiwu, Linong and Lunong intrusions are presented in Table 2. Initial Sr isotopic ratios $(^{87}Sr/^{86}Sr)_i$ values and Nd isotopic parameter $\varepsilon_{Nd}(t)$ values are calculated at t = 230 Ma. The Beiwu granodiorites (six samples) display $(^{87}Sr/^{86}Sr)_i = 0.7087–0.7095$ and $\varepsilon_{Nd}(t) = -5.9$ to −6.2 (Fig. 10A) with $T_{DM2} = 1.49–1.51$ Ga. $(^{87}Sr/^{86}Sr)_i$ values of Linong rocks (five samples) range from 0.7078 to 0.7148, and $\varepsilon_{Nd}(t) = -6.1$

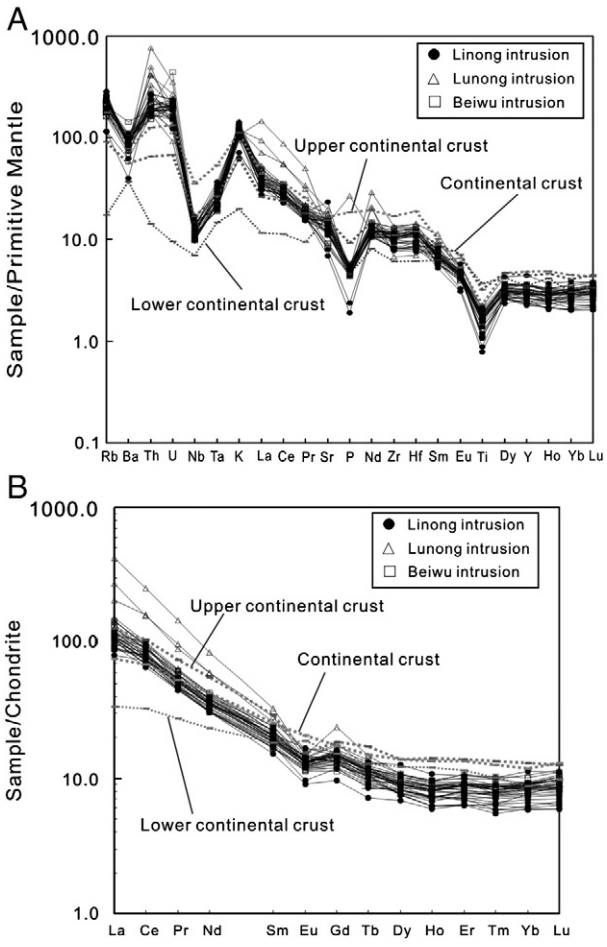

Fig. 8. Primitive mantle-normalized trace element concentrations (A) and chondrite-normalized rare earth element distribution patterns (B) of the Beiwu, Linong and Lunong granitoids. Primitive mantle-normalized values and chondrite-normalized values are from Sun and McDonough (1989). Trace elemental (including REE) compositions of the lower continental crust, upper continental crust and continental crust are also from Sun and McDonough (1989).

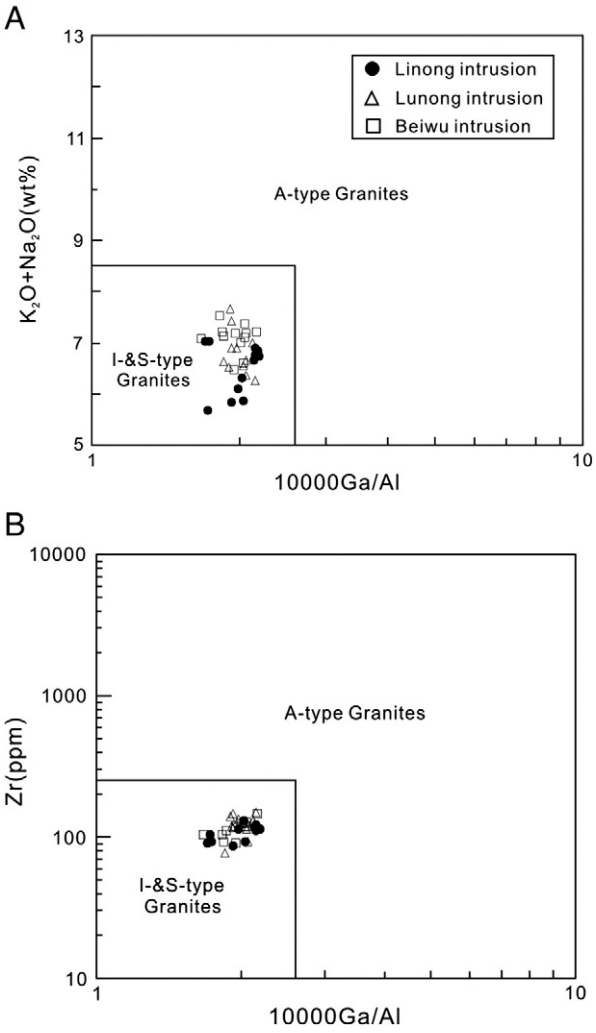

Fig. 9. (A) $K_2O + Na_2O$, (B) Zr vs. 10,000 Ga/Al classification diagrams of the Beiwu, Linong and Lunong granitoids (Whalen et al., 1987).

to −6.7, with T_{DM2} (two-stage Nd model age) = 1.50–1.55 Ga. Comparatively, the Lunong granodiorites (two samples) have higher initial Sr isotopic ratios and lower $\varepsilon_{Nd}(t)$ values, which displays $(^{87}Sr/^{86}Sr)_i = 0.7097–0.7105$ and $\varepsilon_{Nd}(t) = -5.1$ to −5.4 with $T_{DM2} = 1.42–1.44$ Ga. The results suggest that the Beiwu, Linong and Lunong granitoids have consistent Sr and Nd isotopic compositions, indicating that they share a common magma source.

The Beiwu, Linong and Lunong granitoids also have similar Pb isotopic compositions (Table 3). All samples are characterized by high radiogenic Pb isotopic compositions with present-day whole-rock Pb isotopic ratios of $^{206}Pb/^{204}Pb = 18.454–19.196$, $^{207}Pb/^{204}Pb = 15.663–15.748$ and $^{208}Pb/^{204}Pb = 38.793–39.411$. Initial Pb isotopic ratios of the above intrusions at t = 230 Ma are calculated using the whole-rock Pb isotopic ratios and whole-rock U, Th and Pb contents. The calculated initial Pb isotopic ratios are $(^{206}Pb/^{204}Pb)_t = 18.213–18.598$, $(^{207}Pb/^{204}Pb)_t = 15.637–15.730$ and $(^{208}Pb/^{204}Pb)_t = 38.323–38.791$, which are not significantly different from the present-day Pb isotopic ratios (Table 2) as a result of their young age.

6. Discussion

6.1. Fractional crystallization

The systematic decreases in MgO, Fe_2O_3 (total Fe), Al_2O_3, TiO_2 and P_2O_5 with increasing SiO_2 contents for the granitoids in this study, indicate fractionation involving mafic minerals (i.e., amphibole, clinopyroxene), Fe–Ti oxides, feldspars and apatite (Wu et al., 2003; Zhong et al., 2009). Negative anomalies of Nb, Ta and Ti are considered to be related to fractionation of Ti-bearing phase (ilmenite, titanite, etc.). Negative anomalies of P may result from apatite fractionation. Low MgO contents (0.52–1.81 wt.%) are consistent with the fractionation of Mg-rich minerals (i.e., amphibole, clinopyroxene). Moreover, the granitoids have slightly negative anomalies of Eu (most $Eu/Eu^* = 0.65–0.93$) and insignificant anomalies of Sr, indicating insignificant fractionation of plagioclase. Ba depletion requires fractionation of K-feldspar and/or plagioclase. In log–log diagrams (Fig. 11) of Ba vs. Eu/Eu^* and Sr vs. Eu/Eu^*, negative Ba anomalies mainly result from K-feldspar separation, whereas, Sr contents are related to fractionation of minor plagioclase.

6.2. Magma source

As discussed above, I- and S-type granites in the continental crust were thought to be derived from preexisting infracrustal igneous rocks and supracrustal sedimentary rocks (Kemp et al., 2007; Wu et al., 2007; Wyllie, 1977; Zhang et al., 2008b). Recent studies of

Table 2
Rb–Sr, Sm–Nd isotopic ratios for the Beiwu, Linong and Lunong intrusions.

Sample no.	$^{87}Rb/^{86}Sr$	$^{87}Sr/^{86}Sr$	±2σ	$(^{87}Sr/^{86}Sr)_t$	$^{147}Sm/^{144}Nd$	$^{143}Nd/^{144}Nd$	±2σ	$(^{143}Nd/^{144}Nd)_t$	$\varepsilon_{Nd}(t)$	T_{DM1}(Ma)	T_{DM2}(Ma)
The Linong intrusion											
LiN-2	0.430	0.716178	4	0.7148	0.1068	0.512191	7	0.51203	−6.1	1368	1501
LiN-3	3.132	0.718022	4	0.7078	0.1099	0.512187	4	0.51202	−6.3	1415	1515
LiN-4	3.306	0.719900	5	0.7091	0.0980	0.512168	6	0.51202	−6.3	1294	1516
LiN-5	0.716	0.711487	3	0.7091	0.1204	0.512180	4	0.51200	−6.7	1585	1551
LiN-6	0.984	0.712358	3	0.7091	0.1166	0.512194	7	0.51202	−6.3	1502	1520
The Lunong intrusion											
LuN-1	0.840	0.713265	4	0.7105	0.0847	0.512209	5	0.51208	−5.1	1113	1420
LuN-2	1.394	0.714218	4	0.7097	0.0923	0.512206	6	0.51207	−5.4	1187	1443
The Beiwu intrusion											
BW-1	2.160	0.716128	4	0.7091	0.1058	0.512197	4	0.51204	−5.9	1347	1489
BW-2	1.860	0.715142	3	0.7091	0.1097	0.512188	5	0.51202	−6.2	1410	1513
BW-3	1.871	0.714817	7	0.7087	0.1147	0.512197	5	0.51202	−6.2	1468	1511
BW-4	1.440	0.714244	3	0.7095	0.1082	0.512190	6	0.51203	−6.1	1387	1506
BW-5	1.272	0.712874	4	0.7087	0.1070	0.512200	7	0.51204	−5.9	1358	1487
BW-6	2.064	0.715819	5	0.7091	0.1151	0.512202	5	0.51203	−6.1	1466	1503

Note: all the initial isotopic ratios were corrected to 230 Ma. Rb, Sr, Sm and Nd abundances for the samples were determined by ICP-MS. $\varepsilon_{Nd}(t)$ values are calculated using present-day $(^{147}Sm/^{144}Nd)_{CHUR} = 0.1967$ and $(^{143}Nd/^{144}Nd)_{CHUR} = 0.512638$. T_{DM} values are calculated using present-day $(^{147}Sm/^{144}Nd)_{DM} = 0.2137$ and $(^{143}Nd/^{144}Nd)_{DM} = 0.51315$. The details for single- (T_{DM1}) or two-stage (T_{DM2}) Nd model age calculations are given by Wu et al. (2002). Two-stage Nd model age (T_{DM2}) is calculated using the same formulation as Keto and Jacobsen (1987).

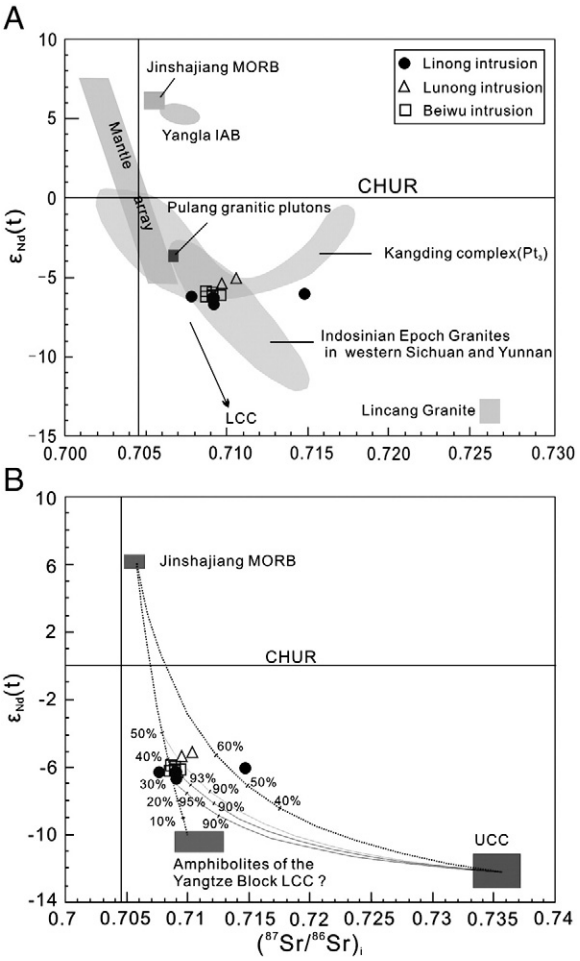

Fig. 10. (A) $\varepsilon_{Nd}(t)$ vs. $(^{87}Sr/^{86}Sr)_i$ diagram of the Beiwu, Linong and Lunong granitoids. The trends of the lower continental crust (LCC) are from Jahn et al. (1999). All the initial isotopic ratios were corrected to 230 Ma. The Yangla island arc basalts (Yangla IAB) are from our unpublished data; the Jinsajiang MORB from Xu and Castillo (2004), IndoSinian Epoch granites in western Sichuan and Yunnan from Zhang et al. (2006, 2007, 2008a), Xiao et al. (2007); and Wang et al. (2008), the Pulang granitic plutons from Pang et al. (2009); Kangding complex from Chen et al. (2001); and the Lincang granites from Liu and Zhu (1989). (B) The simulated diagram of Sr–Nd isotopic mixing. The Jinshajiang MORB represents mantle-derived magmas: $\varepsilon_{Nd}(t)=6.1$, Nd = 7.2 ppm, $(^{87}Sr/^{86}Sr)_i=0.7054$, Sr = 260 ppm. Rocks from the Xiongsong Group (Hao, 1993) are considered as represented melts of the upper continental crust (UCC): $\varepsilon_{Nd}(t)=-12.2$, Nd = 27.6 ppm, $(^{87}Sr/^{86}Sr)_i=0.7357$, Sr = 168 ppm. The amphibolites of the Yangtze Block LCC ($\varepsilon_{Nd}(t)=-10$, Nd = 12 ppm, $(^{87}Sr/^{86}Sr)_i=0.710$, Sr = 260 ppm) are estimated by Gao et al. (1999), Ma et al. (2000) and Zhao et al. (2010).

zircon U–Pb age and zircon Hf and O isotopes indicate that I-type granite can also be generated by the reworking of sedimentary materials that have been modified by mantle-derived magmas (Kemp et al., 2007; Li et al., 2009a). In addition, a three-component (i.e., depleted mantle, the lower crust and upper crust) isotopic mixing model has been proposed to explain the petrogenesis of I- and S-type granites in the Lachlan fold belt (Collins and Richards, 2008; Keay et al., 1997).

As shown in Fig. 8, the samples from the Beiwu, Linong and Lunong granitoids have negative anomalies of HFSEs (Nb, Ta and Ti) and positive anomalies of LILEs in the primitive mantle-normalized spidergrams, consistent with the continental crustal compositions (Rudnick and Fountain, 1995). Furthermore, they have high $(^{87}Sr/^{86}Sr)_i$ ratios, Pb isotopic ratios and $\delta^{18}O$ values and low $\varepsilon_{Nd}(t)$ values, with ancient two-stage Nd and Hf model ages. They were likely derived from anatexis or remelting of ancient continental crust. Very low degree hydrous melting of peridotite could produce andesitic melts, but to produce the observed volumes of felsic melts by peridotite melting is physically difficult and practically unlikely (Fig. 2; Mo et al., 2007). Furthermore, granitic plutons in the Yidun Arc which have similar characteristics to the three intrusions are also interpreted to be derived from melting of a homogeneous crustal source (Reid et al., 2007). It has been shown that elemental ratios, such as Nb/Ta ratios can be very useful in fingerprinting source regions (Eby et al., 1998). Beiwu, Linong and Lunong intrusions have Nb/Ta ratios from 6.1 to 13.3, with an average value of 8.6, which is slightly higher than the ranges of lower crust (Nb/Ta = 8.3; Sun and McDonough, 1989). It is suggested that three granitoids mainly derived from the remelting of the lower crust. However, two aspects have to be addressed. The first question involves whether there is mantle-source magma input. It should be noted that the granitoids possess heterogeneous zircon Hf isotopic ratios of −8.6 to +2.8 (Appendix C; Fig. 12A), similar to the previous analytical results for the Linong intrusion (4.3 to +2.4; Wang et al., 2010). Hf isotopic ratios of the melts parental to zircons are difficult to be reset after its system closed, and they are not modified due to processes of partial melting or fractional crystallization (Bolhar et al., 2008). Therefore, the heterogeneities of zircon Hf isotope are consistent with magma source. As shown in Fig. 12A, the three granitic intrusions possess a wide range of $\varepsilon_{Hf}(t)$ values. The negative $\varepsilon_{Hf}(t)$ values represent the features of the crustal melt, and the positive Hf isotopic ratios are consistent with mantle array (Kemp et al., 2007; Li et al., 2009a; Yang et al., 2007). On the zircon Hf–O isotopic plot (Fig. 12B), there is a clearly negative correlation for the Beiwu, Linong and Lunong intrusions, showing variable involvement of mantle components in their origin (Kemp et al., 2007; Li et al., 2009a). The occurrences of the MMEs provide another evidence for the contribution of mantle-derived magma. The enclaves have crenulate and/or chilled margins. They preserve igneous microtextures, characterized by oscillatory zoning of crystals, euhedral grain shapes, and poikilitic biotite and hornblende in quartz and K-feldspar, indicating crystallization of the enclaves from a melt (Keay et al., 1997). Moreover, SiO_2 contents (53.2–59.9 wt.%) of the MMEs are between the basalts and the host-granitoids, and they have zircon U–Pb ages of 235.9 ± 3.3 Ma, consistent with those three intrusions (unpublished data of the authors). These field and geochemical relations are striking evidence that the enclaves were formed by magma mingling (Vernon et al., 1988). This features also indicate that the felsic and mantle-derived magmas coexisted, mingled, and potentially mixed at deep crustal levels (the lower crust), because it is suggested that efficient magma mixing between mafic and felsic magmas could happen only under the conditions of high temperature and intense magma convection at depth (Chen et al., 2009; Wiebe et al., 1997).

Given that the Beiwu, Linong and Lunong intrusions were derived from two source components (i.e., mantle-derived and lower crustal components), then the high Pb isotopic ratios and elevated $\delta^{18}O$ values of these rocks indicate the presence of a more evolved composition. These granitoids have high radiogenic Pb isotopic compositions [$(^{206}Pb/^{204}Pb)_t = 18.213–18.598$, $(^{207}Pb/^{204}Pb)_t = 15.637–15.730$ and $(^{208}Pb/^{204}Pb)_t = 38.323–38.791$], and all fall above the line of NHRL (Fig. 13; Table 3). It is suggested that both depleted mantle and the lower crust have low radiogenic Pb isotopic compositions [$(^{206}Pb/^{204}Pb)_0 < 18.0$, $(^{207}Pb/^{204}Pb)_0 < 15.5$ and $(^{208}Pb/^{204}Pb)_0 < 37.5$], but the upper crust represented by sedimentary rocks is more radiogenetic (Rollinson, 1993). Thus, the high radiogenic Pb isotopic compositions of these intrusions indicate genetic involvement of sedimentary rocks (Zhang et al., 2006). Oxygen isotopic data provide another striking evidence for a significant contribution of the upper crustal component. $\delta^{18}O$ values of zircon from three intrusions range from 7.3‰ to 9.3‰ (Fig. 5; Appendix B), higher than mantle-derived magma ($\delta^{18}O = 5.3‰ \pm 0.3‰$) and global average value of the lower crust ($\delta^{18}O = 7.0‰$; Pamela et al., 1992), suggesting assimilation of sedimentary rocks.

Table 3
Whole-rock Pb isotopic data of the Beiwu, Linong and Lunong intrusions.

Sample no.	$^{208}Pb/^{204}Pb$	2σ	$^{207}Pb/^{204}Pb$	2σ	$^{206}Pb/^{204}Pb$	2σ	$^{232}Th/^{204}Pb$[a]	$^{238}U/^{204}Pb$[a]	$(^{208}Pb/^{204}Pb)_t$[b]	$(^{207}Pb/^{204}Pb)_t$[b]	$(^{206}Pb/^{204}Pb)_t$[b]
The Linong intrusion											
liN-2	39.21095	39	15.72484	15	18.86182	18	77.2	16.3	38.323	15.695	18.271
liN-3	39.20446	32	15.71817	12	18.87031	14	45.8	9.55	38.678	15.701	18.523
liN-4	39.24684	18	15.72828	7	18.89293	8	39.6	8.11	38.791	15.713	18.598
liN-5	39.07346	46	15.73707	18	18.71588	22	32.0	7.72	38.704	15.723	18.435
liN-6	39.18641	31	15.73414	12	18.71234	15	36.0	5.82	38.772	15.723	18.501
The Lunong intrusion											
LuN-2	39.37439	17	15.74818	7	18.80041	8	80.6	9.80	38.447	15.730	18.444
The Beiwu intrusion											
BW-1	38.96637	43	15.66253	16	18.71580	16	49.3	13.8	38.399	15.637	18.213
BW-2	38.79326	38	15.68869	14	18.45431	17	13.2	3.68	38.642	15.682	18.320
BW-4	39.41141	38	15.68486	15	19.19566	19	67.2	21.0	38.638	15.646	18.432
BW-5	39.03105	22	15.67299	9	18.80011	11	40.9	12.5	38.560	15.650	18.347
BW-6	39.01241	35	15.67732	14	18.75800	17	36.5	11.6	38.592	15.65	18.335

[a] Calculated by measured whole-rock U, Th and Pb contents (Table 1) and present-day whole-rock Pb isotopic ratios.
[b] Initial Pb isotopic ratio at t = 230 Ma.

Two two-component Sr–Nd isotopic mixing models for the three granitoids are shown in Fig. 10B. It has been referred to that the Eaqing Complex is the metamorphic basement of the Jinshajiang Suture, but its isotopic compositions are lacking. Previous studies suggest the Jinshajiang Ocean was a back-arc basin formed after the Changdu–Simao micro-continental Block splitting away from the Yangtze Block in Late Devonion or Early Carboniferous (Metcalfe, 2002; Wang et al., 2000). Accordingly, the Changdu–Simao micro-continental Block should have an affinity with western margin of the Yangzte Block. Pb isotopic data of the Beiwu, Linong and Lunong granitoids provide another line of evidence for the Yangtze (South China) affinity of the Changdu–Simao basement (Fig. 13). High initial Pb isotopic ratios [$(^{206}Pb/^{204}Pb)_t = 18.213–18.598$, $(^{207}Pb/^{204}Pb)_t = 15.637–15.730$ and $(^{208}Pb/^{204}Pb)_t = 38.323–38.791$] of the three granitic intrusions (Table 3; Fig. 13) resemble those of the Yangtze Block (Zhang, 1995), especially the Songpan–Garze Mesozoic granitoids (Zhang et al., 2006). Therefore, the amphibolites of the Yangtze lower crust (Gao et al., 1999; Ma et al., 2000, Zhao et al., 2010) is taken as the lower crustal component. The inferred mantle component is modeled using the Jinshajiang MORB for its basaltic compositions and primitive isotopic signature [$(^{87}Sr/^{86}Sr)_i = 0.7054$, $\varepsilon_{Nd}(t) = 6.1$]. The upper crustal component is taken as the metasediments from the Xiongsong Group ($(^{87}Sr/^{86}Sr)_i = 0.7357$, $\varepsilon_{Nd}(t) = -12.2$; Hao, 1993) in the Batang country of western Sichuan province. The hyperbolic mixing curves suggest that neither the mixing of the lower crustal and mantle-derived components nor the upper crust–mantle mixing could explain the isotopic compositions of the three intrusions (Fig. 10B). It also reveals that 60–70% of the lower crustal components, 25–35% of the mantle-derived compositions and the addition of about 5% of the upper crustal metasediments are sufficient to explain the observed Sr and Nd elemental and isotopic compositions of the three intrusions. In addition, the Indosinian granitoids from western Sichuan and Yunnan province have Sr and Nd isotopic compositions similar to the three intrusions (Fig. 10A), which might have similar magma source. However, more work should be conducted to examine the demonstration.

6.3. Implications for tectonic setting

The Jinshajiang Ocean is an important branch of the Paleo-Tethys Ocean, therefore, its evolution is significant for the whole eastern Paleo-Tethys Ocean. It has been suggested that the Jinshajiang Ocean opened in Late Devonian or Early Carboniferous, and regional collisional event finished before Late Triassic. For the subduction-related events, the Niangjiushan plagiogranites and the Jiyidu granodiorites in the Jinshajiang suture zone yielded SHRIMP zircon ages of 285 ± 6 Ma and 263 ± 6 Ma (Jian et al., 2008), implying that the Jinshajiang oceanic slab subducted westward during the Permian. The Beiwu, Linong and Lunong granitoids have SIMS zircon U–Pb ages of 233.9 ± 1.4 Ma (2σ), 233.1 ± 1.4 Ma (2σ) and 231.0 ± 1.6 Ma (2σ) (Fig. 4), respectively. Therefore, it is conceivable that these granitoids should be related to post-collisional or late collisional event. The studied granitic rocks have initial $^{87}Sr/^{86}Sr$ ratios of 0.7087 to 0.7095 (Fig. 10; Table 2), similar to those of contemporary felsic rocks from the Pantiange Formation felsic

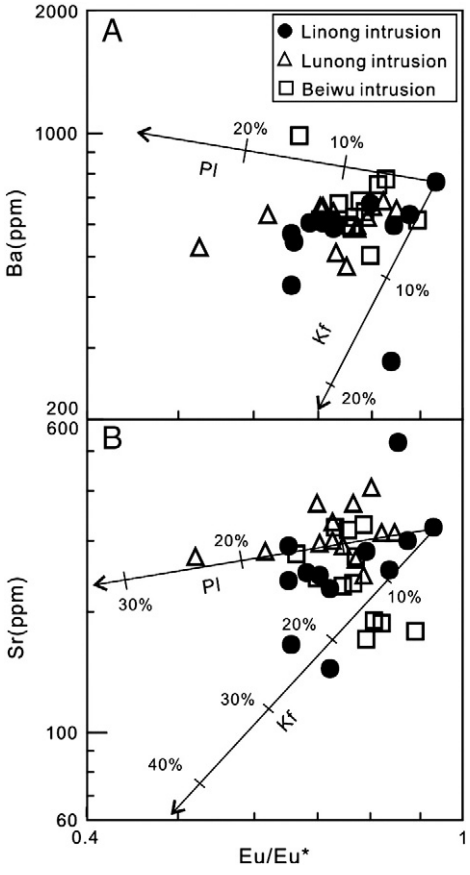

Fig. 11. Eu/Eu* vs. Ba (A) and Eu/Eu* vs. Sr (B) diagrams of Beiwu, Linong and Lunong granitoids. The mineral fractionation vectors, calculated using partition coefficients derive from Arth (1976); the sample with the lowest DI is supposed to be parent melt. The tick marks indicate the percentage of mineral phase removed, in 10% intervals. Kf: K-feldspar; Pl: plagioclase.

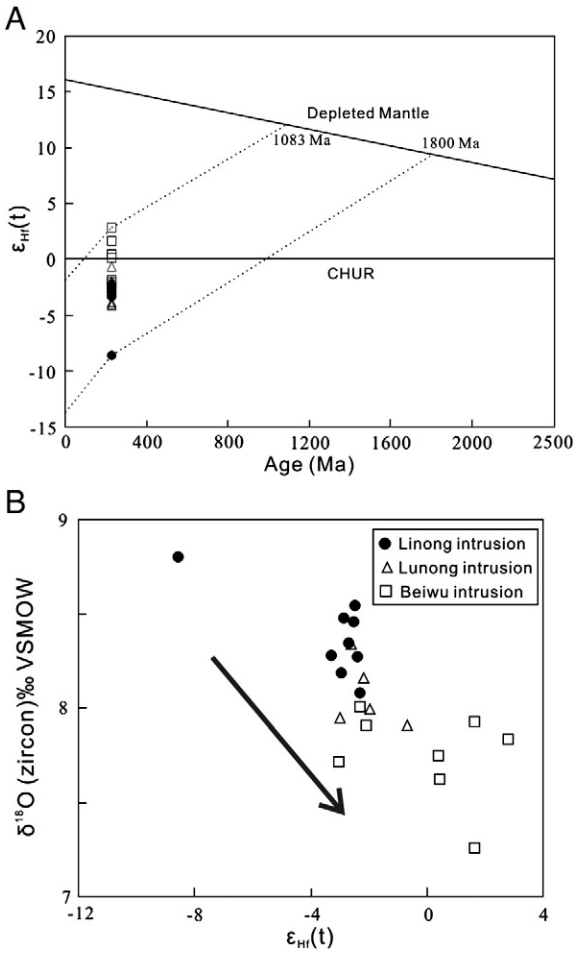

Fig. 12. (A) Diagram of Hf isotopic evolution in the zircons from the Beiwu, Linong and Lunong intrusions. Depleted mantle evolution is calculated by using $\varepsilon_{Hf}(t)=16$ at $t=0$ Ma for MORB at present (Nowell et al., 1998) amd$\varepsilon_{Hf}(t)=6$ at $t=2.7$ Ga (Vervoort and Blichert-Toft, 1999); (B) Plot of Hf vs. O isotopes of zircons from the Beiwu, Linong and Lunong intrusions.

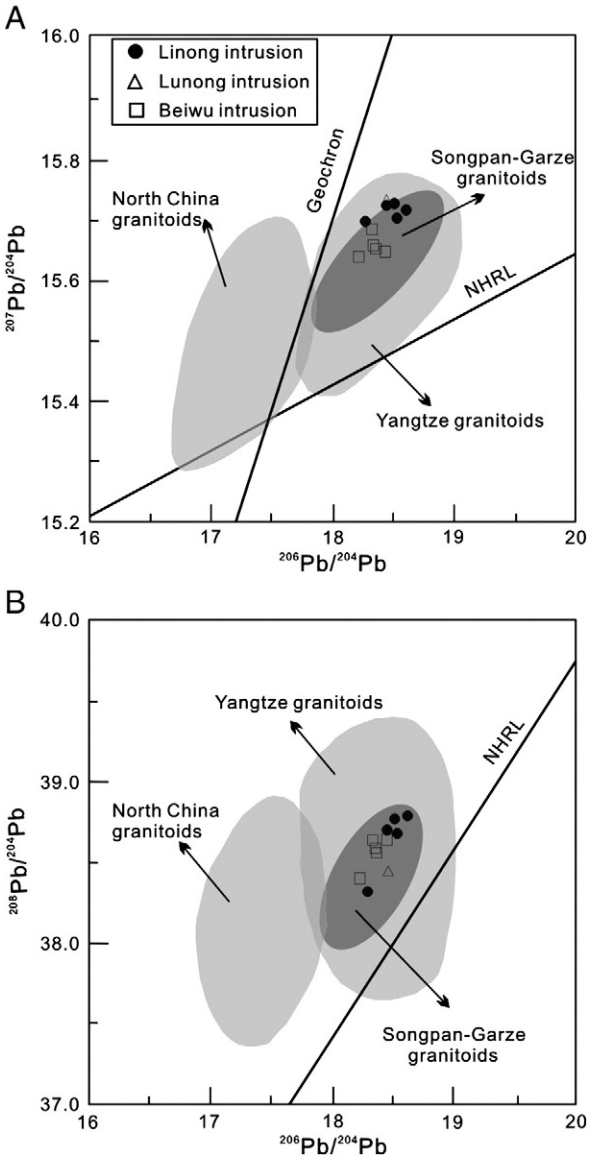

Fig. 13. (A) $^{207}Pb/^{204}Pb$ vs. $^{206}Pb/^{204}Pb$ diagram; (B) $^{208}Pb/^{204}Pb$ vs. $^{206}Pb/^{204}Pb$ diagram. Data of the North China and Yangtze granitoids are from Zhang (1995), which are K-feldspar Pb isotopic ratios of Mesozoic granitoids. Data of Songpan–Garze granitoid are from Zhang et al. (2006, 2007) and Xiao et al. (2007).

rocks in the Lanping basin [$(^{87}Sr/^{86}Sr)_i=0.7072$; Mu and Yu, 2002] and the Luchun–Hongponiuchang Triassic volcanic rocks near the Deqin county [$(^{87}Sr/^{86}Sr)_i=0.7065$–$0.7199$; Wang et al., 2002]. Rocks from both the Lanping basin and Deqin county are bimodal volcanic rocks, indicating that they were generated under a post-collisional tectonic setting. Similarly, among the regional area, the Lincang monzonitic granite and Manghuai Formation felsic volcanic rocks have consistent geochemical characteristics and formation age with the Beiwu, Linong and Lunong granitoids. They have also been interpreted to be produced under a post-collisional or late collisional setting (Peng et al., 2006). Furthermore, in the plots of the tectonic discrimination diagram (Fig. 14), the samples are commonly plotted within the field of late collisional and post-collisional granite. Consequently, the above discussions suggest that the Beiwu, Linong and Lunong granitic intrusions might be generated under a post-collisional or late collisional tectonic setting.

As demonstrated above, the Sanjiang Domain represented by the Jinshajiang suture zone experienced a post-collisional or late collisional event before Late Triassic (possibly at middle Triassic). Underplating of mantle-derived magmas at the crust–mantle boundary is an important way which triggered the crust–mantle mixing (e.g. Bergantz, 1989; Peressini et al., 2007). Therefore, a likely scenario of the petrological process can be described as follows:

Regional decompressed environment induced asthenosphere upwelling, which resulted in the hot mantle-derived melt underplating in the lower crust and thus crustal anatexis. Then, the hybrid melts generated by the mantle-derived and lower crustal magmas, ascended to a shallow depth of the crust and promoted assimilation of sedimentary rocks. Such three-component mixing magmas and subsequent fractional crystallization could be responsible for the formation of the Beiwu, Linong and Lunong granitoids.

6. Conclusions

This study has allowed us to reach the following conclusions:

(1) SIMS zircon U–Pb dating results reveal that the Beiwu, Linong and Lunong granitoids were formed at 233.9 ± 1.4 Ma (2σ), 233.1 ± 1.4 Ma (2σ) and 231.0 ± 1.6 Ma (2σ), respectively, under a late collisional or post-collisional setting, suggesting that the collision was completed before Late Triassic.

(2) The three granitoid intrusions are characterized by quartz, plagioclase and K-feldspar as the principal mineral phases with

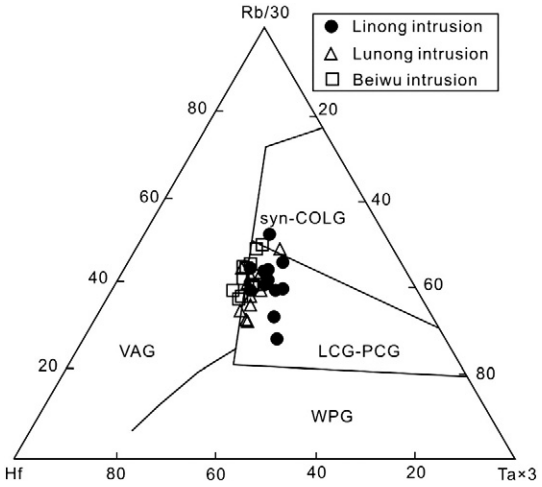

Fig. 14. Rb/30 vs. Hf vs. 3×Ta diagram of the Beiwu, Linong and Lunong granitoids (after Pearce et al. (1984)). Syn-COLG: syn-collisional granites, VAG: volcanic arc granites; WPG: within-plate granites; LCG–PCG: late collisional–post-collisional granites.

minor amounts of hornblende, biotite and some accessory minerals. They are enriched in Si, K, Rb, Th, U, and LREE, and depleted in Nb, Ta, P, and Ti, with insignificantly negative anomalies of Eu, indicating that these granites have undergone fractional crystallization with separation of Ti-bearing phase (ilmenite, titanite, etc.), apatite and K-feldspar. Genetically, they are metaluminous to slightly peraluminous I-type granites.

(3) High initial $^{87}Sr/^{86}Sr$ ratios (0.7078–0.7148) and negative $\varepsilon_{Nd}(t)$ values (−5.1 to −6.7), together with average Nb/Ta ratio of 8.6, variable $\varepsilon_{Hf}(t)$ values (−8.6 to +2.8) and the occurrences of mafic microgranular enclaves, suggest that the Beiwu, Linong and Lunong granitoids originated from hydrid melts, including underplated mantle-derived magmas and the lower crustal magma. Elevated $\delta^{18}O$ values (7.3‰–9.3‰) and relative high Pb isotopic compositions support the presence of the upper crustal sedimentary rocks. Such three-component mixing magmas and subsequent fractional crystallization could be responsible for the generation of the Beiwu, Linong and Lunong granitoids.

Supplementary materials related to this article can be found online at doi:10.1016/j.lithos.2011.07.003.

Acknowledgments

We appreciate the assistance of Profs. Xian-hua Li with U–Pb dating and oxygen isotope analysis by Cameca IMS-1280 SIMS, Ms. Xin Yan with zircon CL imaging, Dr. Xiaoyan Hu in major element analysis by XRF, Ms. Jing Hu for trace element analysis by ICP-MS, and Prof. Lian Zhou for Nd–Sr–Pb isotopes analysis by TIMS. Prof. Quan Wan and Mei-fu Zhou, and Dr. Yun-xing Xue, Zai-cong Wang and Jin-gen Dai are thanked for their constructive reviews of this manuscript. Prof. Ian Metcalfe, an anonymous reviewer and the editor Prof. G. Nelson Eby are thanked for their constructive and valuable reviews of this manuscript. This study was jointly supported by the National Key Basic Research Program of China (2009CB421005), a grant from the Knowledge innovation Program of the Chinese Academy of Sciences (KZCX2-YW-Q04-08; and KZCX2-YW-Q04-01).

References

Arth, J.G., 1976. Behavior of trace elements during magmatic progresses—a summary of theoretical models and their applications. Journal of Research of the United States Geological Survey 4, 41–47.

Bergantz, G.W., 1989. Underplating and partial melting: implications for melt generation and extraction. Science 245, 1093–1095.

Blichert-Toft, J., Albarede, F., 1997. The Lu–Hf geochemistry of chondrites and the evolution of the mantle–crust system. Earth and Planetary Science Letters 148, 243–258.

Bolhar, R., Weaver, S.D., Whitehouse, M.J., Palin, J.M., Woodhead, J.D., Cole, J.W., 2008. Sources and evolution of arc magmas inferred from coupled O and Hf isotope systematics of plutonic zircons from the Cretaceous Separation Point Suite (New Zealand). Earth and Planetary Science Letters 268, 312–324.

Chappell, B.W., 1999. Aluminium saturation in I- and S-type granites and the characterization of fractionated haplogranites. Lithos 46, 535–551.

Chappell, B.W., White, A.J.R., 1992. I- and S-type granites in the Lachlan fold belt. Royal Society of Edinburgh Transactions 83, 1–26.

Chappell, B.W., White, A.J.R., Wyborn, D., 1987. The importance of residual source material (restite) in granite petrogenesis. Journal of Petrology 28, 1111–1138.

Chen, B., He, J.B., Ma, X.H., 2009. Petrogenesis of mafic enclaves from the north Taihang Yanshanian intermediate to felsic plutons: evidence from petrological, geochemical, and zircon Hf–O isotopic data. Science in China Series D: Earth Sciences 52, 1331–1344.

Chen, Y.L., Luo, Z.H., Liu, C., 2001. New recognition of Kangding–Mianning metamorphic complexes from Sichuan, western Yangtze Craton. Earth Science–Journal of China University of Geosciences 26, 279–285.

Clemens, J.D., 2003. S-type granitic magmas—petrogenetic issues, models and evidence. Earth Science Review 61, 1–18.

Collins, W.J., Richards, S.W., 2008. Geodynamic significance of S-type granites in circum Pacific orogens. Geology 36, 559–562.

Eby, G.N., Woolley, A.R., Din, V., Platt, G., 1998. Geochemistry and petrogenesis of nepheline syenite: Kasungu–Chipala, Ilomba, and Ulindi nepheline syenite intrusions, North Nyasa Alkaline Province, Malawi. Journal of Petrology 39, 1405–1424.

Fan, W.M., Peng, T.P., Wang, Y.J., 2009. Triassic magmatism in the southern Lancangjiang zone, southwestern China and its constraints on the tectonic evolution of Paleo-Tethys. Earth Science Frontiers 16, 291–302 (in Chinese with English abstract).

Gao, S., Ling, W.L., Qiu, Y.M., Zhou, L., Hartmann, G., Simon, K., 1999. Contrasting geochemical and Sm–Nd isotopic compositions of Archean metasediments from the Kongling high-grade terrain of the Yangtze craton: evidence for cratonic evolution and redistribution of REE during crustal anatexis. Geochimica et Cosmochimica Acta 63, 2071–2088.

Goodge, J.W., Vervoort, J.D., 2006. Origin of Mesoproterozoic A-type granites in Laurentia: Hf isotope evidence. Earth and Planetary Science Letters 243, 711–731.

Griffin, W.L., Pearson, N.J., Belousova, E., Jackson, S.E., Achterbergh, E., O'Reilly, S.Y., Shee, S.R., 2000. The Hf isotope composition of cratonic mantle: LA–MC-ICPMS analysis of zircon megacrysts in kimberlites. Geochimica et Cosmochimica Acta 64, 133–147.

Griffin, W.L., Wang, X., Jackson, S.E., Pearson, N.J., O'Reilly, S.Y., Xu, X., Zhou, X., 2002. Zircon chemistry and magma mixing, SE China: in-situ analysis of Hf isotopes, Tonglu and Pingtan igneous complexes. Lithos 61, 237–269.

Hao, T.P., 1993. Sm–Nd isotopic ages of Proterozoic metamorphic rocks from the middle sector of the Jinsha River. Geological Review 39, 52–56 (in Chinese with English abstract).

Hou, Z.Q., Qu, X.M., Zhou, J.R., Yang, Y.Q., Huang, D.H., Lü, Q.T., Tang, S.H., Yu, J.J., Wang, H.P., Zhao, J.H., 2001. Collision-orogenic progresses of the Yidun Arc in the Sanjiang region: record of granites. Acta Geological Sinica 75, 484–497 (in Chinese with English abstract).

Hou, Z.Q., Wang, L.Q., Zaw, K., Mo, X.X., Wang, M.J., Li, D.M., Pan, G.T., 2003. Post-collisional crustal extension setting and VHMS mineralization in the Jinshajiang orogenic belt, southwestern China. Ore Geology Reviews 22, 177–199.

Hou, Z.Q., Zaw, K., Pan, G.T., Mo, X.X., Xu, Q., Hu, Y.Z., Li, X.Z., 2007. Sanjiang Tethyan metallogenesis in S.W. China: tectonic setting, metallogenic epochs and deposit types. Ore Geology Reviews 31, 48–87.

Jahn, B.M., Wu, F.Y., Lo, C.H., Tsai, C.H., 1999. Crust–mantle interaction induced by deep subduction of the continental crust: geochemical and Sr–Nd isotopic evidence from post-collisional mafic–ultramafic intrusions of the northern Dabie complex, central China. Chemical Geology 157, 119–146.

Jian, P., Liu, D.Y., Sun, X.M., 2003. SHRIMP dating of Baimaxueshan and Ludian granitoid batholiths northwestern Yunnan provinee, and its geological implications. Acta Geoscience Sinica 24, 337–342 (in Chinese with English abstract).

Jian, P., Liu, D.Y., Sun, X.M., 2008. SHRIMP dating of the Permo-Carboniferous Jinshajiang ophiolite, southwestern China: geochronological constraints for the evolution of Paleo-Tethys. Journal of Asian Earth Sciences 32, 371–384.

Jian, P., Liu, D.Y., Kröner, A., Zhang, Q., Wang, Y.Z., Sun, X.M., Zhang, W., 2009a. Devonian to Permian plate tectonic cycle of the Paleo-Tethys Orogen in southwest China (I): geochemistry of ophiolites, arc/back-arc assemblages and within-plate igneous rocks. Lithos 113, 748–766.

Jian, P., Liu, D.Y., Kröner, A., Zhang, Q., Wang, Y.Z., Sun, X.M., Zhang, W., 2009b. Devonian to Permian plate tectonic cycle of the Paleo-Tethys Orogen in southwest China (II): insights from zircon ages of ophiolites, arc/back-arc assemblages and within-plate igneous rocks and generation of the Emeishan CFB province. Lithos 113, 763–784.

Keay, S., Collins, W.J., McCulloch, 1997. A three-component Sr–Nd isotopic mixing model for granitoid genesis, Lachlan fold belt, eastern Australia. Geology 25, 307–310.

Kemp, A.I.S., Hawkesworth, C.J., Foster, G.L., Paterson, B.A., Woodhead, J.D., Hergt, J.M., Gray, C.M., Whitehouse, M.J., 2007. Magmatic and crustal differentiation history of granitic rocks from Hf–O isotopes in zircon. Science 315, 980–983.

Keto, L.S., Jacobsen, S.B., 1987. Nd and Sr isotopic variations of Early Paleozoic oceans. Earth and Planetary Science Letters 84, 27–41.
King, E.M., Valley, J.W., Davis, D.W., Edwards, G.R., 1998. Oxygen isotope ratios of Archean plutonic zircons from granite–greenstone belts of the Superior Province: indicator of magmatic source. Precambrian Research 92, 365–387.
Lackey, J.S., Valley, J.W., Saleeby, J.B., 2005. Supracrustal input to magmas in the deep crust of Sierra Nevada batholith: evidence from high-$\delta^{18}O$ zircon. Earth and Planetary Science Letters 235, 315–330.
Li, X.Z., Jiang, X.S., 2003. Archipelagic Orogenesis, Metallogenic Systems and Assessment of the Mineral Resources Along the Nujing–Langcangjiang–Jinshajiang Area in Southwestern China. Geological Publishing House, Beijing. 420 pp. (in Chinese).
Li, X.Z., Liu, W.J., Wang, Y.Z., Zhu, Q.W., Du, D.X., Shen, G.F., Liu, C.J., Que, M.Y., Yang, S.H., Li, D.M., Feng, Q.L., 1999. The Tectonic Evolution and Metallogenesis in the Tethys of the Nujiang–Lancangjiang–Jinshajiang Area, Southwestern China. Geological Publishing House, Beijing. 275 pp. (in Chinese).
Li, X.H., Li, Z.X., Li, W.X., Liu, Y., Yuan, C., Wei, G.J., Qi, C.S., 2007. U–Pb zircon, geochemical and Sr–Nd–Hf isotopic constraints on age and origin of Jurassic I- and A-type granites from central Guangdong, SE China: a major igneous event in response to foundering of a subducted flat-slab? Lithos 96, 186–204.
Li, X.H., Li, W.X., Wang, X.C., Li, Q.L., Liu, Y., Tang, G.Q., 2009a. Role of mantle-derived magma in genesis of early Yanshanian granites in the Nanling Range, South China: in situ zircon Hf–O isotopic constraints. Science in China Series D: Earth Sciences 39, 872–887.
Li, X.-H., Liu, Y., Li, Q.-L., Guo, C.-H., Chamberlain, K.R., 2009b. Precise determination of Phanerozoic zircon Pb/Pb age by multicollector SIMS without external standardization. Geochemistry Geophysics Geosystems 10, Q04010.
Liu, C.S., Zhu, J.C., 1989. Quantitative modeling source rocks of Lincang granite batholith, west Yunnan. Acta Petrologica et Mineralogica 8, 1–12 (in Chinese with English abstract).
Liu, Y.-S., Gao, S., Jin, S.-Y., Hu, S.-H., Sun, M., Zhao, Z.-B., Feng, J.-L., 2001. Geochemistry of lower crustal xenoliths from Neogene Hannuoba Basalt, North China Craton: implication for petrogenesis and lower crustal compostion. Geochimica et Cosmochimica Acta 65, 2589–2604.
Lü, B.X., Wang, Z., Zhang, N.D., Duan, J.Z., Gao, Z.Y., Shen, G.F., Pan, C.Y., Yao, P., 1993. Granitoids in the Sanjiang Region (Nujing–Lancangjiang–Jinshajiang Region) and Their Metallogenetic Specialization. Geological Publishing House, Beijing. 328 pp. (in Chinese).
Ludwig, K.R., 2001. User's manual for Isoplot/Ex (rev. 2.49): a geochronological toolkit for Microsoft Excel. Berkeley Geochronology Center, Special Publication, No. 1a. 55 pp.
Ma, C.Q., Ehlers, C., Xu, C.H., Li, Z.C., Yang, K.G., 2000. The roots of the Dabieshan ultrahigh-pressure metamorphic terrane: constraints from geochemistry and Nd–Sr isotope systematics. Precambrian Research 102, 279–301.
Metcalfe, I., 2002. Permian tectonic framework and paleogeography of SE Asia. Journal of Asian Earth Sciences 20, 551–566.
Middlemost, E.A.K., 1994. Naming materials in the magma/igneous rock system. Earth-Science Reviews 37, 215–224.
Mo, X.X., Pan, G.T., 2006. From the Tethys to the formation of the Qinghai–Tibet Plateau: constrained by tectono-magmatic events. Earth Science Frontiers 13, 43–51 (in Chinese with English abstract).
Mo, X.X., Lu, F.X., Shen, S.Y., Zhu, Q.W., Hou, Z.Q., Yang, K.H., Deng, J.F., Liu, X.P., He, C.X., Lin, P.Y., Zhang, B.M., Tai, D.Q., Chen, M.H., Hu, X.S., Ye, S., Xue, Y.X., Tan, J., Wei, Q.R., Fan, L., 1993. Sanjiang Tethyan Volcanism and Related Mineralization. Geological Publishing House, Beijing. 276 pp. (in Chinese).
Mo, X.X., Hou, Z.Q., Niu, Y.L., Dong, G.C., Qu, X.M., Zhao, Z.D., Yang, Z.M., 2007. Mantle contributions to crustal thickening during continental collision: evidence from Cenozoic igneous rocks in southern Tibet. Lithos 96, 225–242.
Mu, C.L., Yu, Q., 2002. The age of volcanic rock of the Pantiange Formation in the Lanping Basin, Yunnan Province. Jounal of Stratigraphy 26, 289–292 (in Chinese with English abstract).
Nowell, G.M., Kempton, P.D., Noble, S.R., Fitton, J.G., Sauders, A.D., Mahoney, J.J., Taylor, R.N., 1998. High precision Hf isotope measurements of MORB and OIB by thermalionization mass spectrometry: insights into the depleted mantle. Chemical Geology 149, 211–233.
Pamela, D., Kempton, Harmon, R.S., 1992. Oxygen isotope evidence for large-scale hybridization of the lower crust during magmatic underplating. Geochimica et Cosmochimica Acta 56, 971–986.
Pan, G.T., Li, X.Z., Wang, L.Q., Ding, J., Chen, Z.L., 2002. Preliminary division of tectonic units of Qinghai–Tiber plateau and its adjacent regions. Geological Bulletin of China 21, 701–707 (in Chinese with English abstract).
Pan, G.T., Xu, Q., Hou, Z.Q., Wang, L.Q., Du, D.X., Mo, X.X., Li, D.M., Wang, M.J., Li, X.Z., Jiang, X.S., 2003. Archipelagic orogenesis, metallogenic systems and assessment of the mineral resources along the Nujing -Langcangjiang -Jinshajiang area in southwestern China. Geological Publishing House, Beijing, pp. 1–420 (in Chinese).
Pang, Z.S., Du, Y.S., Wang, G.W., Cao, Y., 2009. Geological and geochemical feature and petrogenesis of Pulang complex, Yunan Province, China. Geological Bulletin of China 28, 531–537 (in Chinese with English abstract).
Pearce, J.A., Harris, N.B.W., Tindle, A.G., 1984. Trace element discrimination diagrams for the tectonic interpretation of granitic rocks. Journal of Petrology 25, 956–983.
Peng, T.P., Wang, Y.J., Fan, W.M., Liu, D.Y., Shi, Y.R., Miao, L.C., 2006. Early Mesozoic acidic volcanic rocks from the southern Lancangjiang zone: zircon SHRIMP U–Pb geochronology and tectonic implications. Science in China Series D: Earth Sciences 39, 123–132.
Peressini, G., Quick, J.E., Sinigoi, S., Hofmann, A.W., Fanning, M., 2007. Duration of a large mafic intrusion and heat transfer in the lower crust: a SHRIMP U–Pb zircon study in the Ivrea–Verbano Zone (Western Alps, Italy). Journal of Petrology 48, 1185–1218.
Qi, L., Hu, J., Gregoire, D.C., 2000. Determination of trace elements in granites by inductively coupled plasma mass spectrometry. Talanta 51, 507–513.
Qu, X.M., Yang, Y.Q., Li, Y.G., 2004. A discussion on origin of Yangla copper deposit in light of diversity of ore-hosting rock type. Mineral Deposits 23, 431–442 (in Chinese with English abstract).
Reid, A., Wilson, C.J.L., Phillips, D., Liu, S., 2005. Mesozoic cooling across the Yidun Arc, central-eastern Tibetan Plateau: a reconnaissance $^{40}Ar/^{39}Ar$ study. Tectonophysics 398, 45–66.
Reid, A., Wilson, C.J.L., Liu, S., Pearson, N., Belousova, E., 2007. Mesozoic plutons of the Yidun Arc, SW China: U/Pb geochronology and Hf isotopic signature. Ore Geology Reviews 22, 177–199.
Roger, F., Malavieillea, J., Leloupb, P.H., Calassouc, S., Xu, Z., 2004. Timing of granite emplacement and cooling in the Songpan–Garze Fold Belt (eastern Tibetan Plateau) with tectonic implications. Journal of Asian Earth Sciences 22, 465–481.
Rollinson, H.R., 1993. Using Geochemical Data: Evaluation, Presentation, Interpretation. Longman Group UK Ltd., New York. 352 pp.
Rudnick, R.L., Fountain, D.M., 1995. Nature and composition of the continental crust: a lower crustal perspective. Reviews of Geophysics 33, 267–309.
SBGMR (Sichuan Bureau of Geologyand Mineral Resources), 1997. Multiple classification and correlation of the stratigraphy of China (51). Stratigraphy (Lithostratigraphic) of Yunnan Province. China University of Geosciences Press, Wuhan. 416 pp. (in Chinese).
Scherer, E., Münker, C., Mezger, K., 2001. Calibration of the lutetium–hafnium clock. Science 293, 683–687.
Sun, S.s., McDonough, W.F., 1989. Chemical and isotopic systematics of oceanic basalts: implications for mantle composition and processes. In: Saunders, A.D., Norry, M.J. (Eds.), Magmatism in the Ocean Basins. Geological Society Special Publication, London, pp. 313–345.
Sylvester, P.J., 1998. Postcollisional strongly peraluminous granites. Lithos 45, 29–44.
Tang, H.F., Zhao, Z.Q., Huang, R.S., Han, Y.J., Su, Y.P., 2008. Primary Hf isotopic study of on zircons from the A-type granites in Eastern Junggar of Xinjiang, NW China. Acta Mineralogica Sinica 28, 335–342 (in Chinese with English abstract).
Valley, J.W., Chiarenelli, J.R., McLelland, J.M., 1994. Oxygen isotope geochemistry of zircon. Earth and Planetary Science Letters 126, 187–206.
Valley, J.W., Kinny, P.D., Schulze, D.J., Spicuzza, M.J., 1998. Zircon megacrysts from kimbelites: oxygen Isotope variability among mantle melts. Contributions to Mineralogy and Petrology 133, 1–11.
Valley, J.W., Lackey, J.S., Cavosie, A.J., Clechenko, C.C., Spicuzza, M.J., Basei, M.A.S., Bindeman, I.N., Ferreira, V.P., Sial, A.N., King, E.M., Peck, W.H., Sinha, A.K., Wei, C.S., 2005. 4.4 billion years of crustal maturation: oxygen isotope ratios of magmatic zircon. Contributions to Mineralogy and Petrology 150, 561–580.
Vernon, R.H., Etheridge, M.A., Wall, V.J., 1988. Shape and microstructure of microgranitoid enclaves: Indicators of magma mingling and flow. Lithos 22, 1–11.
Vervoort, J.D., Blichert-Toft, J., 1999. Evolution of the depleted mantle: Hf isotope evidence from juvenile rocks through time. Geochimica et Cosmochimica Acta 63, 533–556.
Wang, L.Q., Pan, G.T., Li, D.M., Xu, Q., Lin, S.L., 1999. The spatio-temporal frame work and geological evolution of the Jinshajiang arc–basin systems. Acta Geological Sinica 73, 206–218 (in Chinese with English abstract).
Wang, X.F., Metcalfe, I., Jian, P., He, L.Q., Wang, C.S., 2000. The Jinshajiang–Ailaoshan suture zone, China: tectonostratigraphy, age and evolution. Journal of Asian Earth Sciences 18, 675–690.
Wang, L.Q., Pan, G.T., Li, D.M., Xu, T.R., 2002. The Rb–Sr age determinations of the "bimodal" volcanic rocks in the Luchun–Hongponiuchang superimposed rift basin, Deqin, Yunnan. Tethyan Geology 22, 65–71 (in Chinese with English abstract).
Wang, Q.W., Wang, K.M., Que, Z.Z., Fu, X.F., 2008. Granites in Western Sichuan Province and Its Metallogenesis Series. Geological Publishing House, Beijing. 305 pp. (in Chinese).
Wang, Y.B., Han, J., Zeng, P.S., Wang, D.H., Hou, K.J., Yin, G.H., Li, W.C., 2010. U–Pb dating and Hf isotopic characteristics of zircons from granodiorite in Yangla copper deposit, Deqin Country, Yunnan, Southwest China. Acta Petrologica Sinica 26, 1833–1844 (in Chinese with English abstract).
Wei, J.Q., Zhan, M.G., Lu, Y.F., Chen, K.X., He, L.Q., 1997. Granites in Deqin Yangla copper deposit district, western Yunnan Province. Geology and Mineral Resources of South China 4, 50–56 (in Chinese with English abstract).
Wei, J.Q., Chen, K.X., Wei, F.Y., 2000. Tectonism–magmatism–mineralization in Yangla region, western Yunnan. Geology and Mineral Resources of South China 1, 59–62 (in Chinese with English abstract).
Whalen, J.B., Currie, K.L., Chappell, B.W., 1987. A-type granites: geochemical characteristics, discrimination and petrogenesis. Contributions to Mineralogy and Petrology 95, 407–419.
White, A.J.R., Chappell, B.W., 1977. Ultrametamorphism and granitoid genesis. Tectonophysics 43, 7–22.
Wiebe, R.A., Smith, D., Sturn, M., King, E.M., Seckler, M.S., 1997. Enclaves in the Cadillac Mountain granite (coastal Maine): samples of hybrid magma from the base of the chamber. Journal of Petrology 38, 393–426.
Woodhead, J., Hergt, J., Shelley, M., Eggins, S., Kemp, R., 2004. Zircon Hf-isotope analysis with an excimer laser, depth profiling, ablation of complex geometries, and concomitant age estimation. Chemical Geology 209, 121–135.
Wu, F.Y., Sun, D.Y., Li, H.M., Jahn, B.M., Wilde, S.A., 2002. A-type granites in northeastern China: age and geochemical constraints on their petrogenesis. Chemical Geology 187, 143–173.
Wu, F.Y., Jahn, B.M., Wilde, S.A., Lo, C.H., Yui, T.F., Lin, Q., Ge, W.C., Sun, D.Y., 2003. Highly fractionated I-type granites in NE China (I): geochronology and petrogenesis. Lithos 66, 241–273.
Wu, F.Y., Li, X.H., Yang, J.H., Zheng, Y.F., 2007. Discussions on the petrogenesis of granites. Acta Petrologic Sinica 23, 1217–1238 (in Chinese with English abstract).

Wyllie, P.J., 1977. Crustal anatexis: an experimental review. Tectonophysics 43, 41–71.
Xiao, L., Zhang, H.F., Clemens, J.D., Wang, Q.W., Kan, Z.Z., Wang, K.M., Ni, P.Z., Liu, X.M., 2007. Late Triassic granitoids of the eastern margin of the Tibetan Plateau: geochronology, petrogenesis and implications for tectonic evolution. Lithos 96, 436–452.
Xiao, L., Qi, H., Pirajno, F., Ni, P.Z., Du, J.X., Wei, Q.R., 2008. Possible correlation between a mantle plume and the evolution of Paleo-Tethys Jinshajiang Ocean: evidence from a volcanic rifted margin in the Xiaru-Tuoding area, Yunnan, SW China. Lithos 100, 112–126.
Xu, J.F., Castillo, P.R., 2004. Geochemical and Nd–Pb isotopic characteristics of the Tethyan asthenosphere: implications for the origin of the Indian Ocean mantle domain. Tectonophysics 393, 9–27.
Yang, J.H., Wu, F.Y., Wilde, S.A., Xie, L.W., Yang, Y.H., Liu, X.M., 2007. Tracing magma mixing in granite genesis: in situ U–Pb dating and Hf isotope analysis of zircons. Contributions to Mineralogy and Petrology 153, 177–190.
Zhan, M.G., Lu, Y.F., Chen, S.F., Dong, F.L., Chen, K.X., Wei, J.Q., He, L.Q., Huo, X.S., Gan, J. M., Yu, F.M., 1998. Deqin Yangla Copper Deposit in Western Yunnna Province. China University of Geology Publishing House, Wuhan, pp. 1–163 (in Chinese).
Zhang, L.G., 1995. Block-geology of Eastern Asia Lithosphere—Isotope Geochemistry and Dynamics of Upper Mantle, Basement and Granite. Chinese Science Press, Beijing. 252 pp. (in Chinese with English abstract).
Zhang, H.F., Zhang, L., Harris, N., Jin, L.L., Yuan, H.L., 2006. U–Pb zircon ages, geochemical and isotopic compositions of granitoids in Songpan–Garze fold belt, eastern Tibetan Plateau: constraints on petrogenesis and tectonic evolution of the basement. Contributions to Mineralogy and Petrology 152, 75–88.
Zhang, H.F., Parrish, R., Zhang, L., Xu, W.C., Yuan, H.L., Gao, S., Quentin, G., Crowley, 2007. A-type granite and adakitic magmatism association in Songpan–Garze fold belt, eastern Tibetan Plateau: implication for lithospheric delamination. Lithos 97, 323–335.
Zhang, H.F., Parrish, R., Zhang, L., Xu, W.C., Yuan, H.L., Gao, S., Quentin, G., Crowley, 2008a. Reply to the comment by Zhang et al. on: "First finding of A-type and adakitic magmatism association in Songpan–Garze fold belt, eastern Tibetan Plateau: Implication for lithospheric delamination". Lithos 103, 565–568.
Zhang, Q., Wang, Y., Pan, G.Q., Li, C.D., Jin, W.J., 2008b. Sources granites: some crucial questions on granite study (4). Acta Petrologic Sinica 24, 1193–1204 (in Chinese with English abstract).
Zhao, J.H., Zhou, M.F., Zheng, J.P., 2010. Metasomatic mantle source and crustal contamination for the formation of the Neoproterozoic mafic dike swarm in the northern Yangtze Block, South China. Lithos 115, 177–189.
Zheng, Y.F., Zhang, S.B., Zhao, Z.F., Wu, Y.B., Li, X.H., Li, Z.X., Wu, F.Y., 2007. Contrasting zircon Hf and O isotopes in the two episodes of Neoproterozoic granitoids in South China: implications for growth and reworking of continental crust. Lithos 96, 127–150.
Zhong, H., Zhu, W.G., Hu, R.Z., Xie, L.W., He, D.F., Liu, F., Chu, Z.Y., 2009. Zircon U–Pb age and Sr–Nd–Hf isotope geochemistry of the Panzhihua A-type syenitic intrusion in the Emeishan large igneous province, southwest China and implications for growth of juvenile crust. Lithos 110, 109–128.
Zhou, L., Gao, S., Liu, Y.S., Ling, W.L., Zhang, L., 2007. Geochemistry and implications of clastic sedimentary rocks from the northern margin of Yangtze Craton. Earth Science—Journal of China University of Geosciences 32, 29–38 (in Chinese with English abstract).
Zhu, J., Zeng, P.S., Zeng, L.C., Yin, J., 2009. Stratigraphic subdivision of the Yangla copper ore district, northwestern Yunnan. Acta Geologica Sinica 83, 1415–1420 (in Chinese with English abstract).